Photochemical Degradation of Chlorobenzene

by

Mateusz Sycz

A thesis
presented to the University of Waterloo
in fulfillment of the
thesis requirement for the degree of
Master of Applied Science
in
Chemical Engineering

Waterloo, Ontario, Canada, 2013

AUTHOR'S DECLARATION

I hereby declare that I am the sole author of this thesis. This is a true copy of the thesis, including any required final revisions, as accepted by my examiners.

I understand that my thesis may be made electronically available to the public.

Abstract

Persistent organic pollutants (POPs) are organic compounds of anthropogenic origin that have been linked to the development of cancer, neurobehavioural impairment, and immune system biochemical alterations. These chemicals have various industrial applications as well as acting as pesticides. Dioxins and furans are some of these compounds that are unintentionally produced in combustion and industrial processes. By definition these compounds have 4 common qualities: they are highly toxic, they are resistant to environmental degradation, they are introduced into the air and water where they travel long distances, and they accumulate in fatty tissues.

Photochemical degradation is a method that has been extensively researched in the last few decades. In the aqueous phase it has already been shown to be able to degrade a number of refractory organics, such as dioxins and furans. The ultimate products of this process tend to be carbon dioxide, water, and mineral anions. Air phase work has been also gaining attention in recent decades as a possible alternative to incineration methods in air pollution control. The advantages of photochemical degradation processes are that they can be initiated at low temperatures, are relatively low cost compared to incineration processes, environmentally benign, and have the potential for quick and complete degradation of organic compounds.

The main aim of the research is to investigate the photochemical degradation potential of PCDD/ PCDFs in gaseous air streams as a potential air pollution control technology. In order to do this, the photodegradation reaction kinetics were determined for chlorobenzene as a suitable surrogate for PCDD/PCDFs. Three different photodegradation schemes were employed: direct photolysis, UV/O_3, and UV/H_2O_2. In addition, ozonolysis reaction rates were also determined to evaluate the effects of on the overall photodegradation rates for the UV/O_3 process. Factors such as humidity levels and temperature were investigated to determine their effects on degradation rates.

Temperature and humidity were not greatly influential on the degradation rates of direct photolysis. The degradation rate of chlorobenzene at a temperature of 100°C and high humidity was noticeably reduced, but unchanged at the 10% RH and 60% RH levels for all temperatures.

Ozonolysis of chlorobenzene was negligible at 30°C for all humidity levels. Ozonolysis reactions at the 60°C and 100°C levels were higher than direct photolysis rates and in the 100°C case exceeded the UV/O_3 degradation rates.

Ozone coupled with UV experiments proved to be the most destructive at the low temperature of 30°C and molar ratio of 10:1 ozone to chlorobenzene. There was a clear and positive relationship between the amount of ozone present in the reactor and the degradation rate. At lower ozone to chlorobenzene molar ratios the degradation rates were not much higher than those for direct photolysis of ozone. The 5:1 molar ratio saw a significant increase in degradation rates over the photolysis rates. The fastest degradation rate was achieved for the 10:1 molar ratio and high humidity, which was over 10 times the rate of direct photolysis. In addition, humidity had a noticeably significant positive effect in these reactions.

The effect of temperature on the UV/ozone reaction scheme was determined for the 5:1 ozone to chlorobenzene ratio. Temperature had an interesting effect on the degradation rates at higher temperatures. As the reactor temperature increased, the degradation rates from ozonolysis and UV/O_3 began to converge at 60°C, ultimately leading to the ozonolysis reaction being faster than the UV/O_3.

Exploratory experiments for the H_2O_2 scheme were performed. H_2O_2 had a positive influence on the degradation rate of chlorobenzene and was about 26% higher than the direct photolysis rates. However for similar conditions, the UV/O_3 process had higher degradation rates as was expected from the difference in absorption values between ozone and hydrogen peroxide.

Acknowledgements

This research could not have been done without funding from NSERC.

I would like to thank Dr. William A. Anderson for his supervision, for his help throughout my research, for giving me ideas, and for reviewing and offering corrections to my thesis.

I would like to thank Dr. Carol Moralejo for all her endless experimental and analytical advice and helping to stave off boredom during those long testing times in the lab.

I would like to thank my graduate school colleagues who provided indispensable advice during new beginnings, Drew Higgins, Clark Chen, Ryan Hsu, Jason Wu, Aaron Davis, and Ja-Yeon Choi.

This thesis is dedicated to those who fail, but continue to pursue their goals;

to my family (Mom, Dad, Emily, and Damian) who have always shown patience and helped me through all of the stressful times;

and to my partners in crime, Damian Sycz, Martin Dasko, Omar Ganai, Louis Owen Li, and Justin Batabyal.

Table of Contents

List of Figures

List of Tables

1.0 Introduction

1.1 Preface

The Chemical Revolution has brought about a number of chemicals that have contributed to human well-being. However, many of the chemicals were implemented rather short-sightedly without consideration of their effects on the wider environment. A number of these compounds have since caused long-term health and ecological consequences that were never anticipated. (UNEP, 2005)

Persistent organic pollutants (POPs) are organic compounds of anthropogenic origin that have been linked to the development of cancer, neurobehavioural impairment, immune system biochemical alterations and possibly dysfunction (Government of Canada, 2006a). These chemicals have various industrial applications as well as acting as pesticides. A number of these compounds are produced unintentionally in combustion and industrial processes. By definition these compounds have 4 common qualities: they are highly toxic, they are resistant to environmental degradation, they evaporate and can travel long distances through the air and water, and they accumulate in fatty tissues (UNEP, 2005).

The growing concern of these effects on human populations, especially the transboundary nature of POPs, led to the signing of the Stockholm convention in 2001. The convention identified 12 classes of persistent organic pollutants that were deemed harmful and high priority for emission reduction. Three compounds of interest in this list are polychlorinated dibenzodioxins (PCDDs), polychlorinated dibenzofurans (PCDFs), hexachlorobenzene (HCBz). Canada was one of the first countries to ratify this convention. Although, “currently in Canada, there is no production, use, marketing or trade of any of the intentionally produced POPs listed in the Stockholm Convention, except for the allowable use of existing PCBs in service” (UNEP, 2008)these three pollutants are produced unintentionally in processes such as waste incineration, iron sintering, base metal smelting, and wood pulp (UNEP, 2007; L Zhang, Sawell, Moralejo, & Anderson, 2007).

There is no widely set emission limit for PCDD/PCDFs and emission limits from stationary sources vary based on the best available technologies (BAT) for that particular source. The BAT will depend on the specific process at a particular source. In general, most BATs are able to achieve limits of 0.1 ng ITEQ/Nm^3. This is an ideal value and usually requires optimization of a number of parameters of the particular process as well. (UNEP, 2007)

The available control technologies to prevent the release of unintentionally produced POPs vary in effectiveness. Adsorption on activated carbon and thermal oxidation are the most commonly used. The activated carbon option is the most commonly used and can achieve very high removal efficiencies when coupled with a filter bag system for particulate removal. However, there are some issues with this strategy. This type of treatment technology only transfers the problem from the gaseous phase to the solid phase. The PCDD/PCDFs in the solid phase, usually on particulate matter, must then be treated by a destructive technique. (Everaert & Baeyens, 2004; Finocchio, Busca, & Notaro, 2006)In incineration processes, direct combustion has been the common treatment technology. Temperatures exceeding between 800-1200°C are needed for complete combustion and destruction of the PCDD/PCDFs. Due to the complexities of this type of process, incomplete combustion is always of concern and can actually cause formation of PCDD/PCDFs. The production of other unwanted by-products at these elevated temperatures such as nitrogen oxides is also a concern. (Everaert, Basyens, & Degrève, 2002)

Table 1 is a summary of some PCDD/PCDF control technologies discussed in Article 5 Annex C of the Stockholm Convention. This section of the Convention is designed to help engineers and other technical personnel to implement BATs.

Control Option	PCDD/PCDF removal Efficiency	Co-benefits
Cyclones	Low efficiency	Coarse dust removal
Electrostatic precipitation	Low efficiency	Designed for dust removal
Bag filter	Medium efficiency	Designed for dust removal
Wet scrubber	Medium efficiency	Designed for dust or acid gas removal
Quenching and subsequent high-efficiency wet scrubber	Medium to high efficiency	Simultaneous reduction of dust, aerosols, HCl, HF, heavy metals and SO2
Afterburner	High efficiency	No residues, but quenching of flue gases required
Catalytic oxidation (selective catalytic reaction)	High efficiency; destruction of PCDD/PCDF and other organics	No residues, simultaneous reduction of NOx
Catalytic bag filters	High efficiency	Simultaneous dust removal
Dry absorption in resins (carbon particles dispersed in a polymer matrix)	Depends on the amount of installed material	Selective for PCDD/PCDF; material can be incinerated after use
Fixed bed or circulating fluidized bed reactor, adsorption with activated carbon or open hearth coke	Medium to high efficiency	Simultaneous reduction of various pollutants such as PCDD/PCDF and mercury; material can be incinerated after use
Entrained flow or circulating fluidized bed reactor with added activated coke/lime or limestone solutions and subsequent fabric filter	High efficiency	Simultaneous reduction of various pollutants such as PCDD/PCDF and mercury; material can be incinerated after use

Table 1. Summary of typical PCDD/F treatment technologies as outlined by Annex C of the Stockholm Convention for Best Available Practices (Taken from (UNEP, 2007))

Photochemical degradation is a method that has been extensively researched in the last few decades. In the aqueous phase it has already been shown to be able to degrade a number refractory organics. Compounds such as chlorophenols, chlorobenzenes, chlorinated biphenyls, dioxins and furans have all been shown to degrade in water. The ultimate products of this process tend to be carbon dioxide, water, and mineral anions. (Ray, 2000)

Air phase work has been also gaining attention in recent decades as a possible alternative to incineration methods in air pollution control. Photochemical reactions can be initiated at low temperatures, are relatively low cost, environmentally benign, and have the potential for quick and complete degradation of organic compounds. (Ray, 2000)

There are three main different schemes for photochemical degradation reactions: UV photolysis, UV photooxidation with ozone or hydrogen peroxide, and UV photocatalytic oxidation. The second and third schemes aim to produce highly reactive hydroxyl radicals which can oxidize many organic compounds; these processes tend to be collectively known as Advanced Oxidation Processes or AOPs.

1.2 Scope of Research Project

The main aim of the research is to investigate the photochemical degradation potential of PCDD/ PCDFs in gaseous air streams as a potential air pollution control technology. In order to do this, the photodegradation reaction kinetics of chlorobenzene as a surrogate for the dioxins and furans will be determined. Direct Photolysis will be investigated initially as a benchmark for later tests. The later tests will include the use of ozone and hydrogen peroxide as photooxidants to improve degradation rates.

1.3 Objective of the Current Research

The objective of this project is to determine the effects of different operating parameters on the photodegradation rate of chlorobenzene as a surrogate for PCDD/PCDFs. Chlorobenzene was chosen for its similar structure to PCDD/PCDFs and it being a precursor to dioxin formation (Finocchio et al., 2006) (H. C. Wang, Liang, & Chang, 2011). A number of different parameters were varied to determine reaction schemes with the most promise. The following aspects of the photodegradation were evaluated:

i. Determine the reaction rate constant for direct photolysis of chlorobenzene under different temperature and humidity levels, namely 30, 60, 100°C and 10, 40, 70% Relative humidity.

ii. Determine the reaction kinetics of ozonolysis of chlorobenzene under a variety of conditions and molar ratios.

iii. Determine the degradation kinetics of chlorobenzene in the presence of O_3 coupled with UV light under different temperatures, humidity levels, and molar ratios.

iv. Determine the impact of chlorobenzene degradation rates using H_2O_2 and UV light.

1.4 PCDDs and PCDFs

1.4.1 Overview

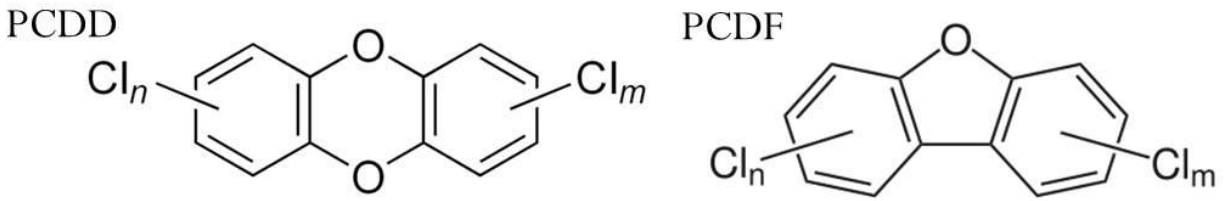

Figure 1. Generic structures of a PCDD and PCDF.

Dioxins and furans are polychlorinated aromatic hydrocarbons that take on the generic structures seen in Figure 1. Of the all possible configurations, 7 of the 75 possible PCDD congeners and 10 of the 135 possible PCDF congeners have "dioxin-like toxicity" (Kulkarni, Crespo, & Afonso, 2008). The PCDFs with these properties have chorine substitution in the 2,3,7,8 positions. Of particular concern are the tetra and higher chlorinated congeners because they can persist in the natural environment for long periods of time. The main natural methods of removal in the atmosphere are photodegradation, hydroxyl radical reactions, and deposition. Photodegradation of gaseous phase dioxins is believed to occur at the soil-air or water-air interfaces (Tysklind, Lindskog, Thaning, Rappet, & Defence, 1993). Those deposited on soil either remain trapped within the soil or are once again released to the atmosphere.

The other more troubling destination for dioxin deposition is in aquatic environments where they are taken up by aquatic animals and bioaccumulate within the ecosystem. The main vector of human exposure is through contaminated food as a result of the bioaccumulation of these substances in the food chain. Foods with higher traces of contaminants are typically foods high in fat: dairy products, eggs, animal fats, and some fish (Travis & Hattemer-Frey, 1991). Developing fetuses and newborn babies are the most sensitive to exposure, usually through their mothers' breast milk. Exposure levels vary on a group's location and dietary habits (Marinković, Pašalić, Ferenčak, Gršković, & Stavljenić Rukavina, 2010). In particular, Canada's Inuit population has high exposure levels due to the colder clime and high fish diet. (Government of Canada, 2006b)

Toxicity Equivalent Factor (TEF)

Toxicity is expressed as toxic equivalent quantities (TEQs) where the most toxic is TCDD (tetrachlorodibenzodioxin) and less toxic compounds are fractions of this.

The biological response of the ingestion of PCDD/PCDFs is difficult to predict due to the fact that a person will be simultaneously exposed to a mixture of congeners. “However, many effects of dioxins are mediated through an interaction with the aryl hydrocarbon receptor. Biological responses include the induction of gene expression of cytochrome P450, CYP1A1, and CYP1A2, disruption of normal hormone signalling pathways, reproductive and developmental defects” (Kulkarni et al., 2008).

Specific detrimental health effects include: soft tissue sarcomas, lymphomes, skin lesions (chloracne), stomach cancer, biochemical liver-test abnormalities, elevated blood lipids, fatal injury, and immune system and neurological effects (Marinković et al., 2010; Mitrou, Dimitriadis, & Raptis, 2001). Other effects have been studied in animals and include: carcinogenic, genetic, reproductive, and development effects. TCDD has an LD50 of 0.04 mg/Kg in rats, others have values of 100 mg/Kg or more (Marinković et al., 2010).

Short term effects of high level exposure to dioxins are damage to liver function and chloracne. Chloracne is a chronic inflammatory skin condition characterised by keratinous plugs with cysts and dark acnes. These mostly appear on the face, but also on the shoulders, back, chest, and the abdomen in severe cases. (Marinković et al., 2010)

Long term exposure leads to effects on the nervous, immune, reproductive, and endocrine systems. Accumulation of TCDD in the body can cause atherosclerosis, hypertension, diabetes, and nervous system damage. The international Agency for Research on Cancer (IARC) and the World Health Organization (WHO) both classify TCDD as a known carcinogen. (Marinković et al., 2010)

1.4.2 Dioxin Sources

Dioxins come mainly from human sources. One study of sediment showed very small levels of dioxins in the soil in 1920, but then concentrations increased since the 1920s as industries grew and more sources came into existence (Alcock & Jones, 1996).

Dioxin sources can be categorized into 4 groups:

(1) Incineration Sources

The largest source of dioxins in the environment is from incineration sources. Of these sources, municipal waste incinerators are the highest producing and most widely studied due to the discovery of dioxins in incinerator fly-ash (Olie, Vermeulen, & Hutzinge, 1977).

There are two main mechanisms of formation: formation from precursors by surface catalyzed processes, and de Novo Synthesis. Other incineration sources include: hospital waste incinerators, hazardous waste incinerators, and sewage sludge incineration. (Kulkarni et al., 2008)

Canadian emissions from this source were 13.173 g ITEQ in 2010 representing 15% of all dioxin/furan emissions. The majority of these emissions were from municipal waste incinerators, representing 74% of the total incineration sources. Another important incinerations source is crematoria emissions. In Canada, this source represented 22% of emissions. (Environment Canada, 2012)

(2) Combustion Sources

An important source of dioxins from combustion processes in open wood burning. In residential settings, wood is usually burned ad hoc without proper aeration. In addition, processed wood is usually treated or varnished with chlorine containing chemicals. This leads to a very viable mixture for dioxin formation. (Lavric, Konnov, & Ruyck, 2004)

In Canada in 2010, residential fuel combustion contributed 5.171 g ITEQ to emissions. This was more than two times the dioxin emissions from electric power generation, 2.501 g ITEQ, which includes coal-fired utility plants. (Environment Canada, 2012)

Another major combustion source is mobile sources, namely diesel trucks and vehicles. In Canada in 2010, there was 8.690 g ITEQ emitted from mobile sources. Light and heavy duty diesel trucks and vehicles represented over 93% of emissions from all mobile sources. (Environment Canada, 2012)

(3) Open and Natural Sources

Dioxins accumulate in soils, sediments, landfill sites, vegetation, and organic matter due to their environmental resistance. This can then recirculate into the environment and be redistributed. The major reservoir sources are biological processes, photochemical processes, accidental sources (such as Seveso, Italy, and Yusho, Japan accidents) as well as forest fires and volcanoes (Kulkarni et al., 2008).

In Canada in 2010, open and natural sources were responsible for 45.756 g ITEQ of emissions, representing over 52% of emissions for that year. The two responsible methods for release were open burning of waste and forest fires (Environment Canada, 2012).

(4) Industrial Sources

Industrial sources are the second most well-known producers of dioxins. This category represents a range of different sources. The more significant industries that produce dioxins are: aluminum production, iron and steel manufacturing, and pulp and paper. Other miscellaneous sources include metal fabrication, glass manufacturing, vehicle manufacturing, electronics, and plastics manufacturing.

In 2010, industrial sources contributed 11.703 g ITEQ of dioxin emissions, representing over 13% of total emissions. Of all the industrial sources the iron and steel industries produced 23%, pulp and paper 18%, aluminum 11%, and miscellaneous industries 27%. (Environment Canada, 2012)

In the metals industry, processes such as high temperature steel production, smelting operations, and scrap metal recovery furnaces emit dioxins (Anderson & Fisher, 2002). Sintering of iron ore has be known to emit dioxins as well (Cieplik et al., 2003; L.-C. Wang, Lee, Tsai, Lee, & Chang-Chien, 2003).

Sintering is a process used in the iron and steel industries to prepare raw material for blast furnaces by fusing together smaller sized materials. The process inputs are iron ore, fluxes, coke for fuel, and recycled materials such as dust and grits. The components are mixed and placed on a large steel conveyor. The mixture is ignited by a series of gas burners with the aid of the coke. This heats the mixture to over 1000°C and causes the bed to fuse together into larger portions. As the conveyor moves, air is drawn through the bed by fans under the conveyor. This causes the bed to cool and harden. It is then ground into small pieces and collected. The cooling waste gas is sent to an ESP to filter any particulate and dusts and then vented out the stack. (Anderson & Fisher, 2002; Cieplik et al., 2003)

The exact mechanism of formation is still not very well known, but is believed that dioxins are formed within the relatively cooler parts of the sinter bed and not within the downstream waste gas as in municipal waste incineration. (Anderson & Fisher, 2002)

Bleached pulp and paper operations can produce dioxins released into water, land, and paper products. These compounds are formed from the chlorination of naturally occurring phenolic compounds in the wood. (Kulkarni et al., 2008)

1.4.3 Current Treatment Technologies

There are a number of different options for treating or controlling PCDD/PCDFs emissions.

Particulate Matter Collection

This method of emission control is based on the principle that PCDD/PCDFs will deposit on particulate matter. The large number of PCDD/PCDFs congeners means they will be split between vapour and particle phases due to the individual physico-chemical characteristics, available particle surface area, and operating temperature. One study using a cloth filter on the flue gas from an iron ore sintering plant yielded a 73% reduction of dioxins (Kulkarni et al., 2008). Another study used an ESP for particulate collection showed removal efficiencies greater than 90% for all dioxin congeners (Karademir, Bakoğlu, & Ayberk, 2003).

Scrubbers and Electrostatic Precipitators

Scrubbers or spray absorber and electrostatic precipitators in combination are an established technology to remove dioxins from flue gas emissions. A lime slurry absorbent is atomized in the spray tower then contacted with the flue gas in a counter-current operation. The gas absorbs into the aqueous phase, then onto the lime solid phase. Due to its basic qualities, it also has the advantage of neutralizing any acidic compounds (i.e. HCl and SO2) (Kulkarni et al., 2008). One study used an ESP followed by two wet scrubbers in series. The first wet scrubber (venture type) removes HCl, HF, heavy metals and organic compounds together with particulate matter. In the second wet scrubber, the flue gas comes into contact with lime solution to remove SO_2 and any remaining pollutants. This control system managed to achieve >99% removal efficiencies of all PCDD/PCDFs. (Karademir et al., 2003). It is important to note, that control of operating temperature is critical as the ESPs themselves can turn into sources of PCDD/PCDFs at temperatures exceeding 250°C (Karademir et al., 2003).

Sorbent Injection

This pollution control scheme involves the injection of finely grained coke from anthracite or bituminous coal mixed with limestone, lime, or inert material into the process waste gas.

PCDD/PCDFs are sorbed onto/into the coke particles. The inert material, which composes up to 80% of the mixture absorbs heat produced from the exothermic nature of the process. This serves two functions: to maintain a constant operating temperature and to prevent the ignition of the coke. The mixture, along with the sorbed contaminants, then settles in a layer on the surface of a bag filter (Cudahy & Helsel, 2000).

Other sorbent materials such as naturally occurring and synthetically produced zeolites have also found use in this method with removal efficiencies reaching over 99% (Abad, Caixach, & Rivera, 2003; Kulkarni et al., 2008).

Fluidized-bed Adsorption

This technology is very similar to the flow injection process in that it works on the same sorption principles, but a fluidized bed of coke is utilized instead of direct injection of the coke into the flue gas stream. The bed is mixed with the same types of inert materials as in the flow injection process to maintain temperature control. However, the fluidized process by nature has very good heat dissipation characteristics and therefore less inert material is needed for temperature control, allowing more coke to be used. Flue gas enters the column from the bottom with sufficient flow velocity to fluidize a particle bed of coke from bituminous coal and inert material with a temperature of 100-120°C. The flue gas then passes through a particle collector (bag filter) and is recirculated to the bed. In addition, fluidized beds offer better contact between gas and adsorbent, so due to these mass transfer conditions, the coke is better utilized. (Kulkarni et al., 2008; Shiomitsu, Hirayama, Iwasaki, Akashi, & Fujisawa, 2002)

Selective Catalytic Reduction

Selective catalytic reduction has been shown to be effective at PCDD/F destruction. In one study a $TiO_2/V_2O_5/WO_3$ type catalyst was used to oxidize PCDD/Fs and NOx. The research showed a destruction efficiency of 99% on average inlet values of 0.1 ng ITEQ/Nm^3 (Goemans et al., 2004). The V_2O_5-WO_3/ TiO_2 catalyst is probably the most promising for applications in PCDD/PCDFs removal. It has a high activity and selectivity with a strong ability in the Cl_2-HCl

environment. It is also very resilient to sulfur dioxide poisoning and effective at selective catalytic reduction of NOx by NH_3 allowing for both organic and inorganic compounds to be treated (Everaert & Baeyens, 2004).

Another group used a TiO_2/V_2O_5 type catalyst. Removal efficiencies of over 98% were achieved for PCDD/PCDFs. The group also noticed a relationship between the operating temperature and removal efficiencies. At 100°C the main mechanism of removal was adsorption, at 150°C it is mainly by destruction, and at 230°C it is entirely destroyed (Liljelind, Unsworth, Maaskant, & Marklund, 2001).

Most catalysts used for PCDD/PCDFs destruction are mostly composed of the oxides of Ti, V, and W. Oxides of Pt and Au supported on silica-boria-alumina have been shown to be effective at 200°C. This method can directly eliminate the compounds without further disposal issues, but lacks the wide spectrum removing capacity of other destructive methods. (Everaert & Baeyens, 2004)

Electron irradiation processes

This method is rather new compared to the other methods and works on principles very similar to photodegradation. The primary route of degradation is by the use of hydroxyl radicals to oxidize the PCDD/PCDFs. Instead of employing ultraviolet light, the hydroxyl radicals are produced from ionizing radiation. The reactive components are formed from the main constituents of air, N_2, O_2, CO_2, and H_2O (Gerasimov, 2001). Studies have shown destruction efficiencies of over 99%. (Kulkarni et al., 2008)

1.5 UV and PCDD/PCDFs

The use of photolysis and photo-oxidants has been studied extensively for the treatment of contaminated water in both industrial and municipal water purification applications (Bhowmick & Semmens, 1994; Ray, 2000). Research in the use of this technology for the treatment of contaminated air has been increasing in the last 15 years (Chou, Huang, & Chang, 2005; Pengyi, Fuyan, Gang, Qing, & Wanpeng, 2003; Shen & Ku, 1998, 1999). A number of authors have

studied the effects of photolysis on PCDD/PCDFs. These studies have mainly focused on light wavelengths over 300 nm. Choi et al discovered that wavelengths of over 300 nm had no impact on the photolysis of four different PCDDs in their system (Choi, Hong, Chang, & Cho, 2000). Another group, Wagenaar et al, measured the photolysis kinetics of octachlorodibenzofuran and octachlorodibenzo-p-dioxin in a number of different solvents including water and concluded that both compounds were susceptible to photolytic degradation with the furan being more photochemically unstable than the dioxin (Wagenaar, Boelhouwers, De Kok, & Groen, 1995). A number of other studies have corroborated this phenomenon (Choudhry & Webster, 1989; Crosby, Moilanen, & Wong, 1973; Dobbs & Grant, 1979; Hung & Ingram, 1990; Hutzinger, Safe, Wentzell, & Zitkhe, 1973; Miller, Hebert, Miille, Mitzel, & Zepp, 1989; Quass, Fermann, & Bröker, 2004)

Chlorobenzene was chosen as the model compound for the research because of its similar structure to PCDD/PCDFs and it being a precursor to dioxin formation mainly by heterogeneous catalytic reactions on fly ash particles (Dickson, Lenoir, & Hutzinger, 1992; Finocchio et al., 2006; H. C. Wang et al., 2011). In addition, there are a number of experimental complexities in working with PCDD/PCDFs in a laboratory setting. PCDD/PCDFs are not very volatile at low temperatures, so introduction into the gas phase would entail working with extremely low concentrations, which would require specialized equipment for handling and analysis (Lavric, Konnov, & De Ruyck, 2005). Furthermore, the photooxidation reaction rates constants in the atmoshphere for 2,3,7,8 –TCDD are within the range of chlorobenzene (atmospheric photooxidation half-life, 2,3,7,8 –TCDD: 22.3–223 hours, chlorobenzene: 72.9–729 hours) (Mackay, Shiu, Ma, & Lee, 2006) and so the results of photochemical degradation experiments with chlorobenzene are expected to provide a reasonable estimate of what would occur with PCDD/PCDFs.

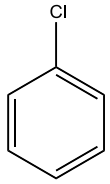

Figure 2. Chemical structure of a chlorobenzene molecule.

2.0 Fundamentals of Photochemistry

All electromagnetic radiation inherently possesses energy. The amount of energy is related to its specific wavelength and is determined from the following relation:

$$E = hv = \frac{hc}{\lambda}$$

In the above equation, E is energy, *h* is Planck's constant (6.626×10^{-34} J s), *c* is the speed of light 2.998×10^{8} m s^{-1}), *v* is the frequency (nm^{-1}), and λ the wavelength of light (nm).

The energies possessed by photons neatly correspond to the bond energies in molecules. The extent of energy absorption is related to the molecular/bond structure. Table 2 shows the relation between different chemical bonds (chromophores) and absorption behaviour (Ray, 2000).

Chromophore	λ_{max} (nm)	Molar Absorptivity (L $mol^{-1}cm^{-1}$)	Transition
C-H or C-C	180	1000	σ→π*
C=C	180	10 000	π→ π*
C=C-C=C	220	20 000	π→ π*
Benzene	260	200	π→ π*
Naphthalene	310	200	π→ π*
Anthracene	350	10 000	π→ π*
Phenol	275	1500	π→ π*
C=O	280	20	n→ π*
C=C-C=O	320	50	n→ π*
C=N	220	20	n→ π*

Table 2. Wavelength of maximum absorption and molar absorptivity for common organic bonds. (Ray, 2000)

Volatile organic compounds absorb electromagnetic radiation rather well due to the presence of one or more double bonds involving carbon, oxygen, or nitrogen.

Once a compound absorbs a photon and becomes electronically excited, it can release this extra energy to return to the ground state in a variety of photophysical deactivation processes or photochemical pathways.

(1) **Dissociation** ($AB^* \rightarrow A + B$)

The energy of the photon was high enough that the molecular bond is broken and the original molecule is broken into fragments (also known as photolysis)

(2) **Intermolecular Reaction** ($AB^* + C \rightarrow AC + B$, or $AB^* + C \rightarrow ABC$)

The excited molecule has enough energy to overcome an activation barrier or the new electronic arrangement is conducive to reaction. Another limited case is intramolecular reaction. An excited area of a molecule may react with another part of the same molecule. This leads to the production of new products or structural rearrangements of the same molecule.

(3) **Isomerization** ($AB^* \rightarrow BA$)

This usually occurs in molecules with cis-trans isomers, where the electronic excitation allows the molecule to rotate around the double bond.

(4) **Ionization** ($AB^* \rightarrow AB^+ + e^-$)

The incident radiation has so much energy that an electron is ejected from its molecular orbit (e.g. photoelectric effect).

(5) **Intermolecular Energy Transfer** ($AB^* + CD \rightarrow AB + CD^\dagger$)

An excited molecule collides with another molecule and the excitation is transferred to the new molecule.

(6) **Luminescence** ($AB^* \rightarrow AB + h\nu$)

The molecule releases the excitation energy as radiation.

(7) **Physical Quenching** ($AB^* + M \rightarrow AB + M$)

The molecule loses its energy to a molecule M where the energy is converted to translational or vibrational forms of energy.

Quantum Yield

The quantum yield of a photochemical system is a measure of the reaction efficiency in relation to the amount of radiation absorbed. It can be defined a number of ways depending on the reference event, whether the reactants are of interest or specific photoproducts. In addition, the primary process of a photochemical system is usually defined as the reactions leading from the initial absorption of radiation by the target molecule. This definition explicitly ignores secondary reactions after those initiated from the initial absorption reaction products. Therefore, the primary quantum yield is defined as "the ratio of the number of molecules undergoing energy absorption to the number of photons absorbed" (Ray, 2000). Depending on the particular compounds and the photochemical system, it is generally accepted that advanced oxidation processes that are photo-initiated tend to involve numerous secondary reactions due to the number of radical species formed (Oppenländer, 2003). Then the primary quantum yield is no longer the best representation of the efficiency of the photochemical system.

The overall quantum yield is the ratio on the total decomposition of the target compounds, which includes the primary process (i.e. photo-initiated reactions) and the subsequent secondary reactions (i.e. radical reactions), to the amount of light absorbed. This metric is highly system dependent and lacks the intrinsic properties of the primary quantum yield (Carlos, Brandi, & Alfanot, 1996). The quantum yield is also dependent on the particular wavelength of the incident radiation. Thus, a system utilizing polychromatic light would need multiple quantum yields.

3.0 Photodegradation Review

3.1 Direct Photolysis

One mechanism of degradation utilizing ultraviolet radiation in both aqueous and gas phases is direct photolysis of the target compound. This occurs when the amount of photonic energy corresponds to the energy level of one of the molecular bonds of the compound. The bond breaks and the molecule fragments and/or becomes radicalized leading to further reactions. A number of studies have been conducted on photolysis of organic compounds in air. Shen et al did an extensive study on 3 different classes of organic compounds, chloromethanes, chloroethanes, and aromatics. All compounds studied showed photolytic activity: dichloromethane, chloroform, carbon tetrachloride, 1,2-dichloroethane, 1,1,1- trichloroethane, 1,1,2,2-tetrachloroethane, benzene, toluene, and o-xylene (Shen & Ku, 1999). Other studies of volatile organic compounds showing photolytic activity in the gaseous phase: chloroform (Bhowmick & Semmens, 1994; Chen, Yang, Pehkonen, & Ray, 2004; Feiyan, Pehkonen, & Ray, 2002; Haag, Johnson, & Scofield, 1996) carbon tetrachloride (Bhowmick & Semmens, 1994; Chen et al., 2004; Feiyan et al., 2002), trichloroethylene (Bhowmick & Semmens, 1994; Feiyan et al., 2002; Lee & Lee, 2005; Shen & Ku, 1998; Wekhof, 1991), tetrachloroethylene (Bhowmick & Semmens, 1994; Lee & Lee, 2005; Shen & Ku, 1998), benzene (Haag et al., 1996; J. Wang & Ray, 2000; Wekhof, 1991), toluene (Jeong, Sekiguchi, & Sakamoto, 2004; J. Wang & Ray, 2000), *cis*-1,2-dichloroethylene (J. Wang & Ray, 2000) and 1,1-dichloroethylene (Haag et al., 1996; Shen & Ku, 1998), 1, 1,2-tricholorethane (Bhowmick & Semmens, 1994), propylene glycol monomethyl ether acetate (Chou, Huang, & Chang, 2006), vinyl chloride, benzene, and dichloromethane (Haag et al., 1996).

Aromatics are more susceptible to photolysis due to their larger cross sections and alkyl substitutions. Direct photolysis can only be achieved by the absorption of radiation with wavelengths between 175 nm and 300 nm (Wekhof, 1991). Referring to the chromophore table in the previous section, Table 2, the exact wavelength needed will depend on the specific bonds within the molecule.

3.2 Oxidation Reactions

Apart from direct photolysis, another mechanism of photodegradation is by using compounds that generate oxidants that oxidize the target compounds. The most effective oxidizing compound is the hydroxyl radical.

3.2.1 Ozone with UV

Ozone is a chemical reagent that has been in use for over 100 years in water treatment. It is a powerful oxidant and known for its disinfection properties, however, it is very selective in its oxidation reactions. It is most useful for cleaving the multiple bonds in aromatic compounds, but these reactions tend to proceed slowly. In water treatment applications, ozone reacts with alicyclic taste and odour compounds such as geosim and methylisoborneol (Glaze, Kang, & Douglas, 1987), aliphatic halides, such as the THMs (Hoigne & Bader, 1983)(Glaze, Peyton, Lin, Huang, & Burieson, 1982) and chlorinated benzenes (Hoigne & Bader, 1983).In combination with ultraviolet light, ozone can be used to produce highly reactive hydroxyl radicals.

The photolysis of ozone in humidified air produces hydroxyl radicals in a two-step process (Finlayson-Pitts & Pitts, 1986):

(1) $O_3 + h\nu \rightarrow O_2 + O(^1D)$ (wavelength ≤ 320 nm)

(2) $O(^1D) + H_2O \rightarrow 2OH^{\bullet}$ (k = 2.2e-10 cm^3 $molecule^{-1}$ sec^{-1} @ 298K)

This is a well-known process that occurs in atmospheric oxidation reactions especially in the troposphere. Reaction 2 is at the same time in competition with the deactivation of $O(^1D)$ by air (Finlayson-Pitts & Pitts, 1986):

(3) $O(^1D) + M \rightarrow O(^3P) + M$ (k = 2.9e-11 cm^3 $molecule^{-1}$ sec^{-1} @298K)

At 1 atm pressure and 298K, only about 10% of the $O(^1D)$ atoms react with water molecules to produce hydroxyl radicals (Finlayson-Pitts & Pitts, 1986).

The rate of reaction with H_2O is given by:

$$-\frac{d[\mathrm{O(1D)}]}{dt} = k_1[\mathrm{H2O}][\mathrm{O(1D)}]$$

The rate of deactivation is given by:

$$-\frac{d[\mathrm{O(1D)}]}{dt} = k_2[\mathrm{M}][\mathrm{O(1D)}]$$

The proportional fate of the hydroxyl radicals at a certain temperature and pressure can be determined from the ratio of these two rate equations.

Two other significant reactions that can also occur between the $O(^1D)$ and H_2O (Finlayson-Pitts & Pitts, 1986):

(4) $$\mathrm{O(\ ^1D) + H_2O \rightarrow O(\ ^3P) + H_2O}$$

(5) $$\mathrm{O(\ ^1D) + H_2O \rightarrow O_2 + H_2}$$

The quantum yield of reaction (1) for a range of wavelengths from 248 nm to 290 nm can be seen in Table 3. Of specific note, the quantum yield at 254 nm is approximately 0.92.

Photolysis Wavelength	Quantum Yield ($O(^1D)$)
290	0.95
274	0.9
271	0.92
230-280	1
266	0.9
254	0.92
248	0.91

Table 3. Absolute Quantum yields of $O(^1D)$ from the Photolysis of O_3. (Adapted from (Finlayson-Pitts & Pitts, 1986))

In addition, the high molar absorption coefficient of ozone at 254 nm (3020 L M^{-1} cm^{-1}) makes using ozone in conjunction with low pressure mercury lamps ideal for $O(^1D)$ generation.

Once the hydroxyl radicals are produced in a photochemical system, they begin a number of reactions.

In the UV/O_3 system the hydroxyl radicals initiates the following reactions (Yu & Lee, 2007):

(6) $RH + OH^{\bullet} \rightarrow ROH_2^{\bullet}$ (chain initiation)

(7) $RH + OH^{\bullet} \rightarrow R^{\bullet} + H_2O$ (chain initiation)

Oxygen is also involved in the reactions (Bhowmick & Semmens, 1994):

(8) $RH + O_2 \rightarrow R^{\bullet} + HO_2^{\bullet}$ (chain initiation)

(9) $R^{\bullet} + O_2 \rightarrow RO_2^{\bullet}$

(10) $RO_2^{\bullet} + RH \rightarrow ROOH + R^{\bullet}$ (chain propagation)

All of the radicals begin extensive chemical reaction.

The loss of hydroxyl radicals from the main reactions occurs by the following (Bhowmick & Semmens, 1994; Ray, 2000):

(11) $OH^{\bullet} + \text{wall} \rightarrow \text{chain termination}$

(12) $OH^{\bullet} + O_3 \rightarrow HO_2^{\bullet} + O_2$

(13) $OH^{\bullet} + O_3 \rightarrow H_2O + O_2$

(14) $O + OH^{\bullet} \rightarrow O_2 + H$

(15) $OH^{\bullet} + OH^{\bullet} \rightarrow H_2O + O$

3.2.2 Hydrogen Peroxide with UV

Another widely used oxidant in photochemical systems is hydrogen peroxide. There are numerous studies of its applications to decontamination and disinfection of a number of compounds and bacteria of a number in the treatment of aqueous effluent of a number of installations. It is not widely used in gas-phase applications due its low vapour pressure. It also has a low molar absorption coefficient which increases with decreasing wavelength in the 300-200 nm range. See Figure 3 for comparison between gaseous and aqueous phase absorption. (Bolton & Cater, 1994)

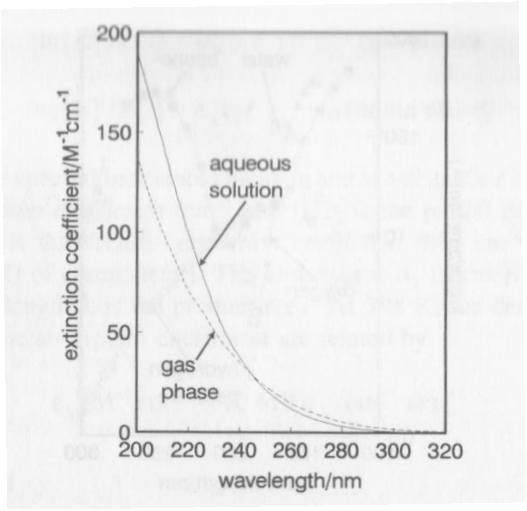

Figure 3. Absorption spectra of hydrogen peroxide in gas and aqueous phases (taken from (Bolton & Cater, 1994)).

However, unlike the mechanism of hydroxyl prediction from ozone, the photolysis of hydrogen peroxide directly produces hydroxyl radicals by the following reaction scheme:

(16) $H_2O_2 + h\nu \rightarrow 2OH^{\bullet}$ (chain initiation)

The hydroxyl radical then engages in propagation reactions to produce more radicals:

(17) $OH^{\bullet} + H_2O_2/HO_2^{\bullet} \rightarrow HO_2^{\bullet}/O_2^{\bullet} + H_2O$

(18) $HO_2^{\bullet} + H_2O_2 \rightarrow OH^{\bullet} + H_2O + O_2$

The chain reaction will terminate thusly:

(19) $HO_2^{\bullet} + HO_2^{\bullet} \rightarrow H_2O_2 + O_2$

The quantum yield of the initiation reaction is 1.0 (Bolton & Cater, 1994).

3.2.3 UV Photocatalysis

Another photoreaction scheme that utilizes UV light to treat contaminant effluent is photocatalytic oxidation. Photocatalytic oxidation is a heterogeneous process that uses solid catalysts that are “activated” by UV light; the activated catalyst then initiates photooxidation. The most commonly used photocatalyst is titanium dioxide, primarily in the anatase form.

Compared to other photocatalysts such as ZnO, ZnS, CdS, Fe_2O_3, and WO_3, TiO_2 exhibits the fastest degradation rates and stability. (Ray, 2000)

Titanium dioxide photocatalysis is initiated by absorption of long UV light. The photonic energy of the absorbed light needs to match the band gap energy, the energy needed for electrons to transfer from the valence band to the conduction band. This electron jump creates a hole in the lower band and a free electron in the conduction band. These holes are very strong oxidizing agents and the electrons can be involved in reduction reactions. (Ray, 2000)

The photocatalytic oxidation steps can be summarized by:

(20) $$\mathrm{TiO_2} + h\nu \rightarrow \mathrm{h_{cb}^+} + \mathrm{e_{cb}^-}$$

(21) $$\mathrm{h_{cb}^+} + \mathrm{H_2O_{(ads)}} \rightarrow \mathrm{OH^-} + \mathrm{H^+}$$

(22) $$\mathrm{h_{vb}^+} + \mathrm{O_{(ads)}^-} \rightarrow \mathrm{OH^\bullet} + \mathrm{H^+}$$

This photooxidation scheme was not investigated in this research, however one of the main mechanisms in air phase photocatalytic degradation research is hydroxyl radical attack. The main mechanism for UV/O_3 oxidation is through hydroxyl radical attack, therefore it is useful from a mechanistic perspective to compare results from these two schemes.

3.3 UV Light Sources

The following section provides an overview of UV lamp technology used in advanced oxidation processes.

The rate of reaction is equal to the light absorbed by the photoreactive species multiplied by the quantum yield (Bolton & Cater, 1994):

$$-\frac{dC_A}{dt} = I\Phi$$

An obvious criterion is that the lamps spectral output must overlap with the absorbance spectrum of the target species. Many pollutants absorb light in the region between 200 and 300 nm. In addition, ozone absorbs very strongly at the 254 nm band. There are four main types of lamps used for advanced oxidation systems:

- Low pressure mercury lamps
- Medium pressure mercury lamps
- Pulsed xenon flash lamps
- Proprietary lamps

(1) Low Pressure Mercury Lamps

Low pressure mercury lamps operate at low pressures (0.1 torr) and temperatures (typically around 40°C). Low pressure mercury lamps have electrical power inputs that range from 9-120W, have lifetimes of 4000 to 10 000 hours, and have relatively high electrical to radiant power conversions of 40-60% (Oppenländer, 2003). The main spectral output of these lamps is centered on 253.7 nm (approximately, 90% radiant output) with less significant output at 185 nm (Bolton & Cater, 1994). They are the most common lamp used in UV disinfection due to its primarily emitting wavelength matching up with the energy needed to cleave DNA in microorganisms. Temperature can affect the radiant output significantly. An optimal electrical energy input exists for every ambient temperature to produce maximum irradiance. Maximum electric power input is limited to less than 300W; due to the high dependency of radiant output

on temperature, higher electric inputs require temperature control and make them impractical (Oppenländer, 2003).

These lamps consist of an outer bulb with an inner quartz arc tube which contains a small amount of high purity mercury and a noble gas such as argon, neon, xenon, or krypton. The materials of the outer bulb and inner arc tube vary upon the intended application. The outer bulb is usually made of quartz, but using high quality synthetic quartz (Suprasil) allows for 184.9 nm to pass through as well (these are so-called ozone producing lamps). The mercury atoms are excited by an electric discharge between either end of the lamp. A high voltage is needed to initially vaporize the mercury, but after initial vaporization, the resistance between the two electrodes decreases until the voltage available strikes the main arc. This main arc vaporizes the remaining mercury. The resistance across the arc between the two electrodes decreases as more mercury vaporizes. All mercury lamps are considered negative resistance devices and require a special ballast to regulate supply current, or they would destroy themselves (Rabek, 1982). The electronically excited mercury atoms return to their ground state by emitting radiation (in the form of ultraviolet light).

(2) Medium Pressure Mercury Lamps

These lamps operate with more mercury than low pressure variants, and thus have higher operating pressures and temperatures. The bulb temperatures are typically in the 400-600°C range and higher. The wavelength range extends from the UV region to the infrared. These lamps typically operate at 1 atmosphere or more and have the following radiant efficiencies UV (29-38%), Vis (15%), and IR (47-55%), but not continuously. Operating lifetimes are between 3000-4000 hours. (Rabek, 1982)

There are a couple of advantages of medium pressure lamps over low pressure variants. Firstly, they can be operated at much higher energy inputs than low pressure lamps, up to 30 kW, but at the expense of electrical to radiant power efficiency (30 to 40%). This translates to higher radiant powers. In addition, in stark contrast to low pressure lamps, medium pressure lamps are relatively temperature independent and can operate at much higher power densities.

One very important consideration in designing any AOP technology is the longevity of the lamp. The irradiance of mercury arc lamps decreases over time. This is mainly due to the mercury reacting with the physical components of the lamp. This aspect must be incorporated into the design to maintain proper decontamination levels. (Oppenländer, 2003)

(3) Pulsed Xenon Flashlamps

The lamps function differently from mercury lamps. These lamps are pulsed rapidly by applying an intense burst of energy. Higher current densities increase the UV output to a theoretical maximum of 28%, although practical applications see output at around 20%. This high operating current reduces the lifetime of the lamp, typically 50-500 hours. (Rabek, 1982)

Xenon flash lamps see some more limited use in AOP applications than mercury lamps. They radiate over a broad continuum from UV to IR and are operated at electrical power inputs of around 3 kW. The main reason for lack of wide spread adoption of these lamps is the cheap, readily available energy from natural sunlight which produces a similar radiation continuum.

(4) Proprietary Lamps

Some photochemical systems manufacturers produce their own lamps, based on medium pressure mercury lamps. These lamps have higher current densities and for comparable power inputs give improved efficiency and spectral emission. Operating temperatures are between 700-1000°C and can emit strongly below 240 nm. (Rabek, 1982)

4.0 Experimental and Methods

4.1 Chlorobenzene Analysis

Chlorobenzene was chosen as the model compound for the research because of its similar structure to PCDD/PCDFs and it being a precursor to dioxin formation mainly by heterogeneous catalytic reactions on fly ash particles (Dickson et al., 1992; Finocchio et al., 2006; H. C. Wang et al., 2011). In addition, there are a number of experimental complexities in working with PCDD/PCDFs in a laboratory setting. PCDD/PCDFs are not very volatile at low temperatures, so introduction into the gas phase would entail working with extremely low concentrations, which would require specialized equipment in handling and analysis. Chlorobenzene is easily introduced into the gas phase and can be quickly analyzed using GC detection. Chlorobenzene was purchased from Sigma-Aldrich (USA) and used without further purification. The UV absorption spectrum of chlorobenzene can be seen in Figure 4.

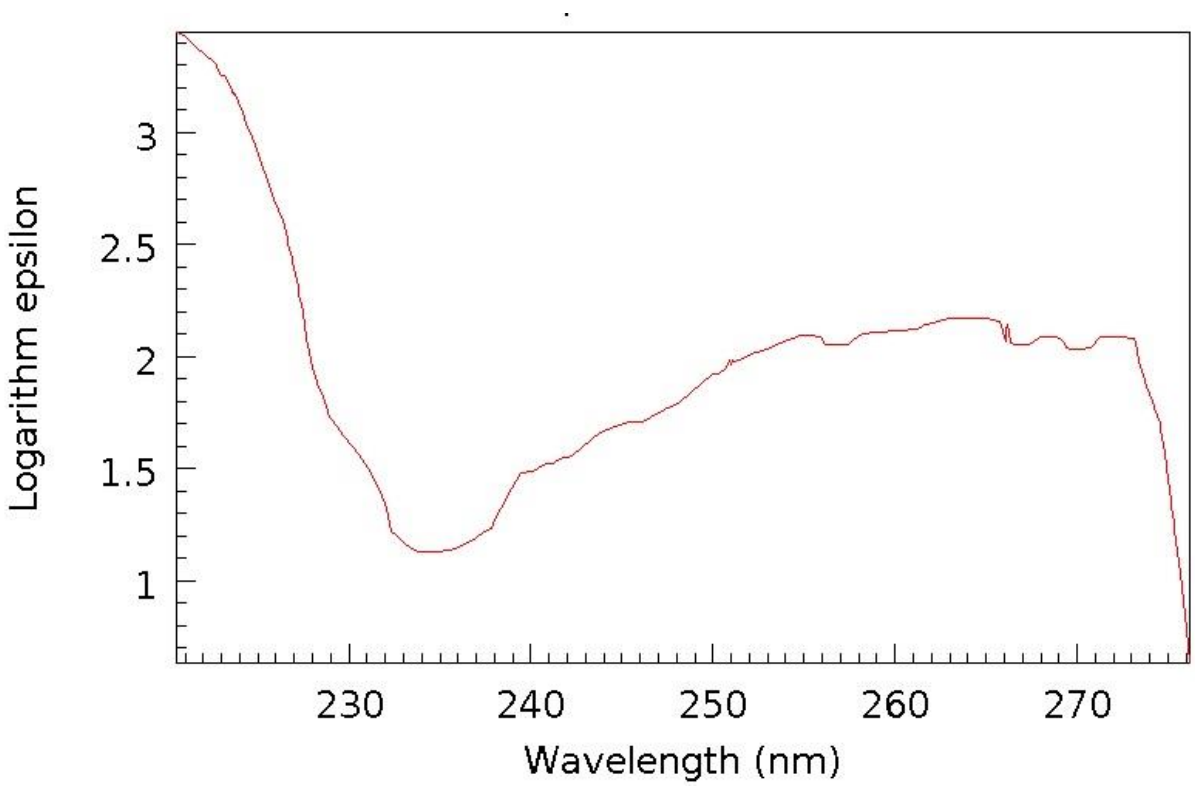

Figure 4. UV absorption spectrum of chlorobenzene. (take from (Grammaticakis, 1949)**)**

Chlorobenzene was analyzed by gas chromatography by using a GC (HP5890 Series II) equipped with a FID detector with a 30 m by 0.53 mm RTX502.2 column (Restek, Pennsylvania). An isothermal temperature program was employed with an oven temperature of 120°C set for 3 minutes. Injector temperature was 250°C and the detector was set for 300°C. Under these conditions, the chlorobenzene had a residence time of approximately 0.9 seconds.

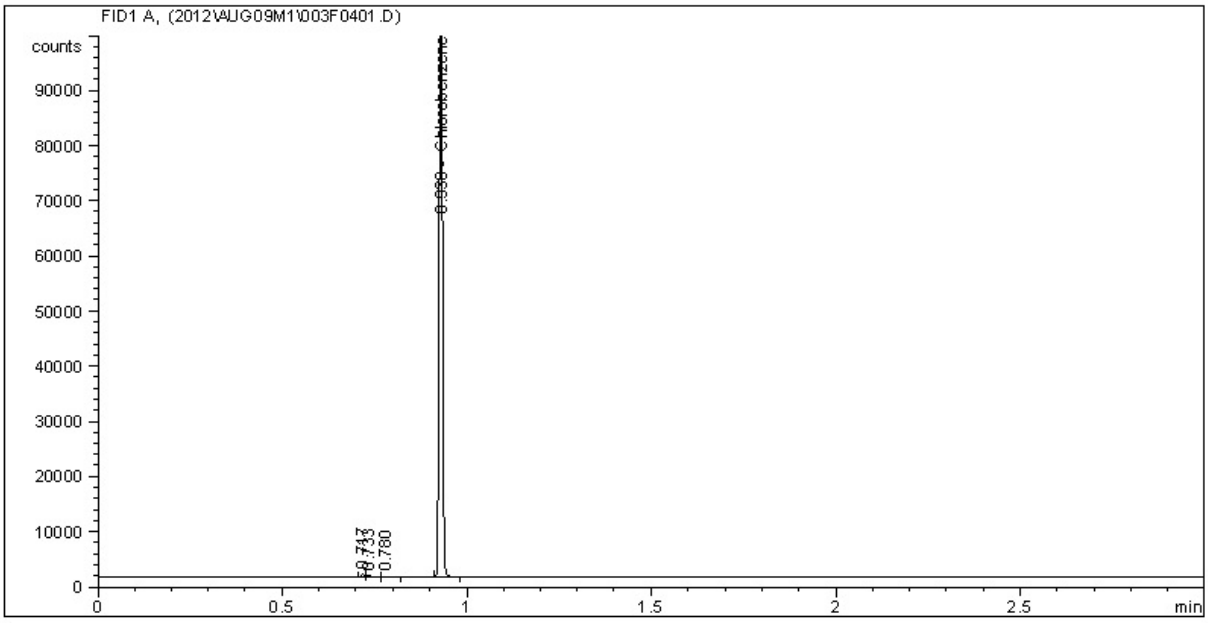

Figure 5. Gas Chromatograph sample output.

A 4 point calibration was employed. A 2 L custom made round bulb with stirring bar embedded was used to prepare an 1110 ng/mL gas phase solution, by injecting 2 µL of liquid chlorobenzene into dry air and allowing it to vaporize. After injection, the contents of the bulb were allowed to mix for 30 minutes. Different volumes of this standard solution were then withdrawn using a gas-tight syringe and injected into the GC. At least 3 injections were performed at every level to ensure accurate area counts. The volumes for calibration gas injected were 1 mL, 500 µL, 200 µL, and 100 µL to produce 1110 ng/mL, 555 ng/mL, 222 ng/mL, 111 ng/mL concentrations respectively.

4.2 Reactor

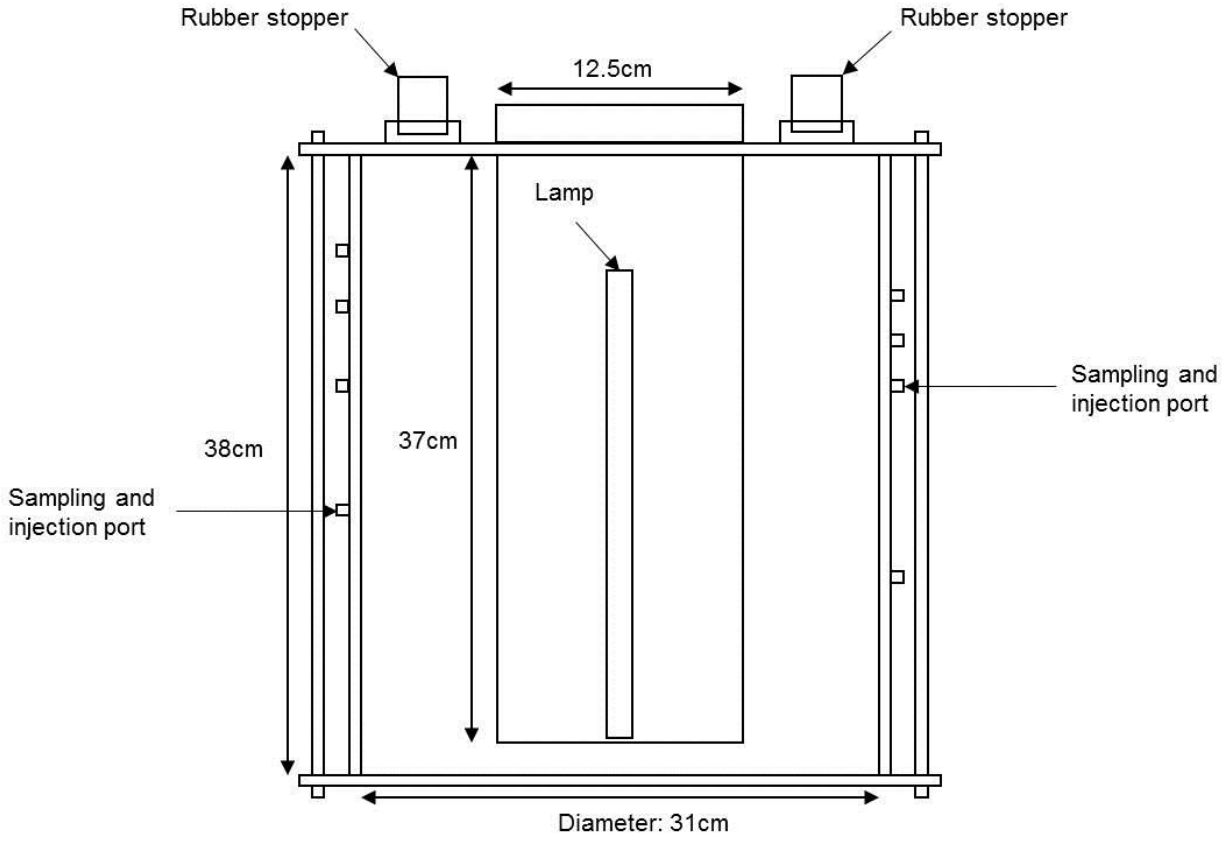

Figure 6. Reactor without external recirculation loop.

The reactor used was a 22L cylindrical vessel composed of an aluminum body and steel top and bottom plates. A quartz cylinder was fitted concentrically through the top plate and joined to the steel with silicone sealant. A 1 cm clearance was intentionally made between the quartz cylinder and the bottom plate to prevent possible breakage of the glass when the cylinder was removed and replaced for cleaning.

The reactor had eight ports of stainless steel National Pipe Thread (NPT) to Swagelok fittings. Two ports were used for chlorobenzene injection and sampling and were fitted with rubber septa and compressed to ensure an air tight seal. The other ports were capped. All NPT fittings were installed with Teflon pipe tape and tested with leak test solution to ensure air tightness.

On top of the reactor were 2 openings that were plugged with rubber stoppers. One opening contained a thermocouple used for temperature measurement and was fitted tightly through

the centre of the rubber stopper. The other opening was plugged with a solid rubber stopper during experiments and unplugged for reactor purging.

The surfaces joining the main body with the top and bottom lids were sealed with two Viton O-rings fitted into grooves in the top and bottom edges of the main aluminum body. Eight pull rods secured the top and bottom lids of the reactor and were fastened by wing nuts.

A Philips TUV16W 4P-SE (16W linear lamp 324mm long, with 4 pins on one end) was used to produce irradiation at 254 nm.

4.3 Photolysis Experiments

Before any experiments were performed, the reactor was flushed with plant air for 45-60 minutes. After about 8-10 photolysis experiments, the reactor was rinsed with water or methanol to remove any non-volatile polar solvent soluble products. At the beginning of every experiment, 15 µL of liquid chlorobenzene was injected into the reactor through one of the rubber septa. A 1 mL sample was immediately withdrawn from the reactor by a gas-tight syringe and injected into the GC. Samples were taken every 5 minutes and injected into the GC.

4.4 Ozone Experiments

The ozone experiments were performed with a slightly different experimental set-up. An external loop was added to recirculate the reacting medium through a 5 cm quartz cuvette. This recirculation is necessary for spectrophotometric measurement of the ozone gas. The external loop was composed of two lines of Viton tubing; one from the reactor to the cuvette and the other from the cuvette through the peristaltic pump then back to the reactor. The tubing was connected to the reactor with 2 stainless steel hose barb to NPT fittings. Viton tubing was chosen due to its excellent resistance to ozone degradation.

Ozone absorption was measured by spectrophotometry by using a spectrophotometer (Ocean Optics USB2000+UV-VIS, USA) and then converted into concentration using the Beer-Lambert Law with an absorption coefficient at 254 nm of 3020 L mol^{-1} cm^{-1} taken from literature (Chen et al., 2004). Chlorobenzene also absorbs at this wavelength, as the photolysis experiments

showed, however the absorption coefficient is significantly less than that for ozone, at 139.6 L mol^{-1} cm^{-1} (Lianfeng Zhang & Anderson, 2013), and can be considered negligible for the concentration levels. Ozone was generated on site using an ozone generator (Ozomax, Quebec).

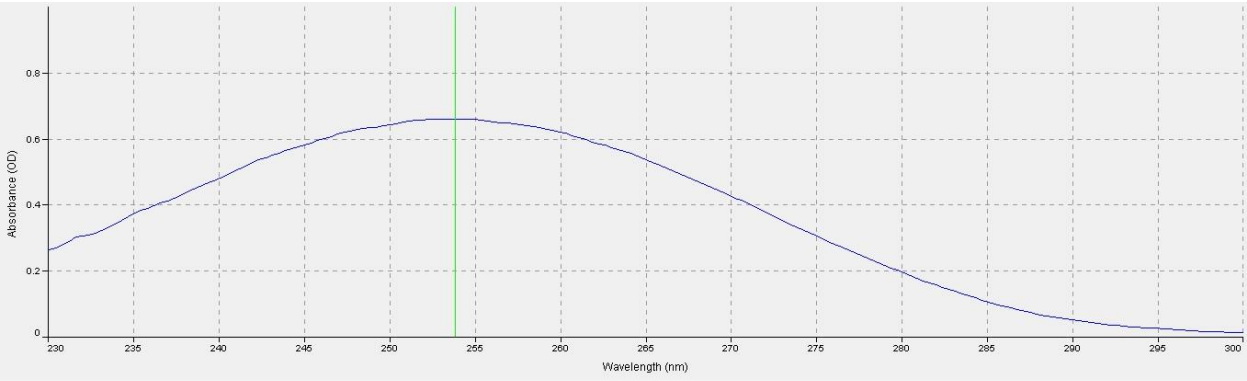

Figure 7. Spectrometer sample output for ozone absorbance.

4.5 Temperature Control

Temperature in the reactor was regulated by a temperature controller and 2 pieces of heating tape wrapped around the base of the cylindrical part of the reactor. A type J thermocouple was used to measure the temperature. Due to the slow response dynamics of the system, only proportional control was used with a small gain constant. This was to minimize temperature overshoot to reach a steady state temperature value quicker. For higher temperature experiments, fibreglass insulation was wrapped around the reactor to minimize heat loss. Before all experiments, temperature steady state values were first achieved before any compounds were introduced into the reactor.

4.6 Irradiance Measurement

Irradiance measurement was accomplished using an Ocean Optics radiometer (with the use of a complementary light source, this device was also used for spectrophotometric measurements). The radiometer uses a charge coupled device to measure the intensity of light and was calibrated using a 2 lamp standard; for the UV region a deuterium lamp and for the IR region a

halogen lamp. To measure the irradiance in the reactor, the radiometer probe was fitted onto a long thin needle that was able to penetrate into the reactor through one of the side ports. Radiometric measurements were made starting at the outer wall of the quartz glass then at 1 cm intervals to the inner wall of the reactor body. The height of the probe corresponded to the middle of the lamp (6 cm).

4.7 Humidity Measurement and Control

Humidity in the reactor was adjusted two different ways. The first way was to run dry air through columns of water, which was then fed into the reactor. A hygrometer with probe was then used to determine relative humidity and steady state values. The other method employed, due to temperature limitations of the available hydrometer of 90°C, was the use of psychrometrics to determine the exact amount of water needed to be injected per reactor volume. Once injected the water was allowed to mix with the other components for 10 minutes before experiments were begun. The relative humidity values were specifically chosen to minimize any condensation that would occur when the reacting mixture was recirculated thought the external loop.

4.8 Hydrogen Peroxide Experiments

Due to the extremely low volatility of hydrogen peroxide, hydrogen peroxide was introduced into the reactor as an aerosol using a Collision Nebulizer. 30% w.t. H_2O_2 solution was poured into the Collision Nebulizer and plant air was fed into the device. The aerosol was then flowed through the reactor and allowed to mix for different periods of time. Gravimetric analysis was used on the H_2O_2 solution to determine a rough estimate of inlet feeds. Due to technical difficulties and lack of special equipment, no specific methods were utilized to determine actual concentrations of the H_2O_2 in the air.

5.0 Results and Discussion

5.1 Irradiation Measurements

Irradiance measurements were taken of the lamp at the three different operating temperatures. This was to determine if the irradiance was similar for all reactor temperatures since it was difficult to control the lamp surface temperature inside the quartz sleeve and the irradiance has been known to be temperature dependent for low pressure mercury lamps (Bolton & Cater, 1994).

The temperature dependence of the irradiance was determined for the 3 different reactor temperatures. The lamp temperature was measured on the glass surface near the top electrode. The results can be seen in Figure 8.

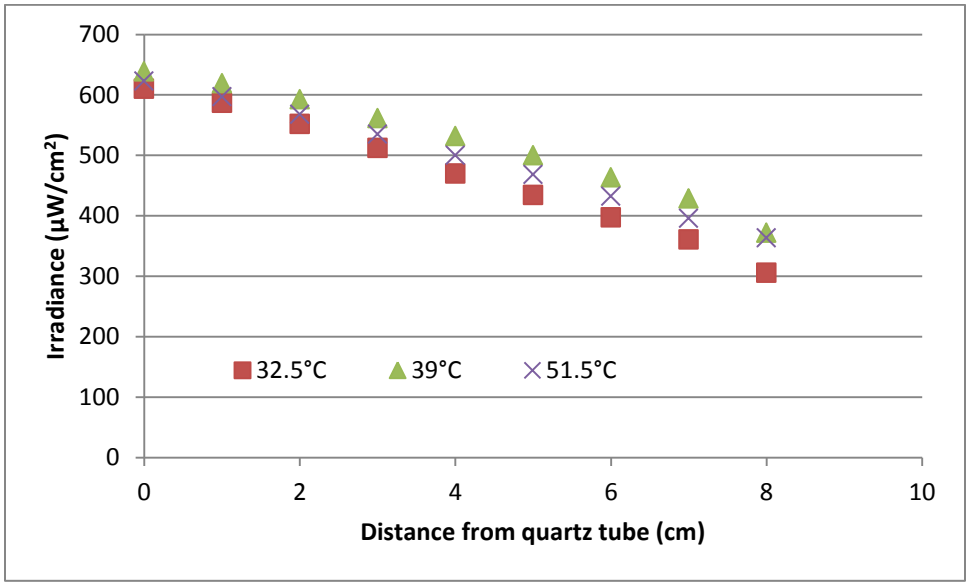

Figure 8. Irradiance variation in the reactor at the three different reactor temperatures.

The average irradiances in the plane of measurement for the three temperatures were 470, 523, and 498 µW/cm^2. It follows from theory, that the lamp temperature has an effect on the irradiance in Low Pressure Mercury lamps and that the optimum temperature is around 40°C as was observed (Bolton & Cater, 1994).

5.2 Direct Photolysis

A number of experiments were performed to evaluate the photodegradation potential of chlorobenzene. Firstly, experiments were performed to determine the suitability of the reactor. That is, to determine the interactions, if any, between the materials of construction of the reactor and chlorobenzene and any small leaks in the reactor where chlorobenzene may diffuse. Figure 9 is a sample of one of these relationships. For the most part there was an interaction between the reactor materials and chlorobenzene. As can be seen in Figure 9, these background effects have a negative relationship on the concentration.

This turned out to be the most troublesome part of the research. Initially, the chlorobenzene concentration was rather consistent during background effects checks. However, as experiments continued, especially when the photolysis and photo-oxidant reactions progressed, the background effects began to increase. Eventually, these background degradation values reached a maximum. In addition, any time a new physical component was introduced into the system, for example when the external loop was being implemented, the components contributed to new instability in the background concentration profile. The literature is very sparse on this phenomenon, but the likely cause is interactions with the reactor materials and the intermediate products of the reactions. The reactor materials then become activated and are then involved in the reaction mechanism. The evidence of this is when the reactor was unused for an extended period of time. When experiments were performed after a 3 month hiatus, the background degradation kinetics were completely different, mainly the chlorobenzene concentration was completely stable with no degradation during background tests for 120 minutes.

One study of the catalytic degradation of chlorobenzene in the presence of iron oxide showed some activity between the chlorobenzene and iron oxide, albeit at higher temperatures (>200°C) and a significantly less exposure time (87s space velocity) compared to the exposure times employed in this study (H. C. Wang et al., 2011). However, due to the complex nature of the radical chain reaction induced during chlorobenzene photolysis and UV/O_3 photooxidation, this could have added to the catalytic effect of the iron oxide. The trend below clearly shows a

significant relationship between chlorobenzene and the reactor, most likely any iron oxidized in the top and bottom plates. This phenomenon made reproducibility for some experiments extremely difficult.

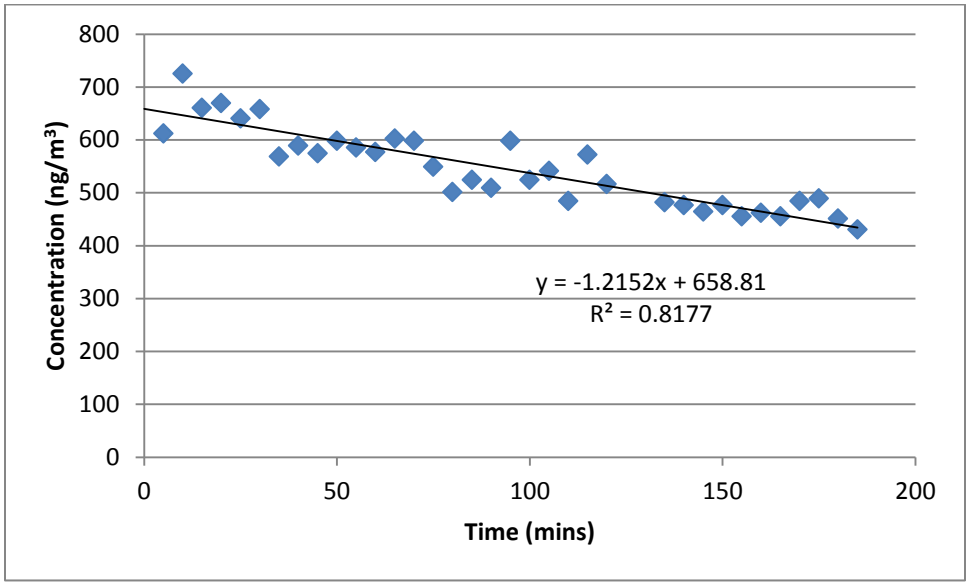

Figure 9. Chlorobenzene concentration profile in reactor over time at 30°C, 10% RH, with no UV.

The relationship can be assumed to be linearly negative, owing to the high coefficient of determination. By applying a first order reaction model and performing linear regression, we obtain Figure 10.

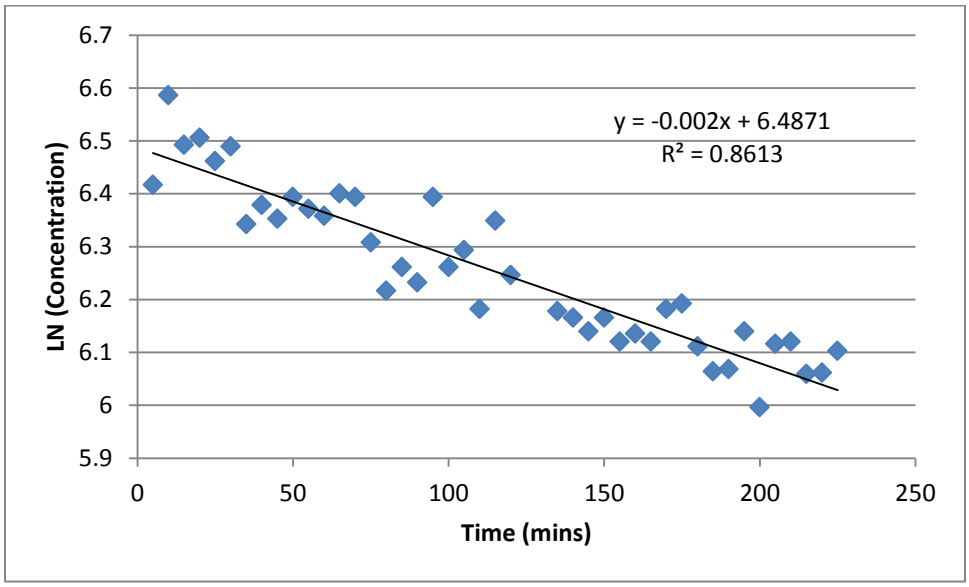

Figure 10. Natural log of concentration versus time of the background effects.

This relationship is also clearly negative due to a high coefficient of determination and a first order reaction model as a reasonable approximation. The slope obtained from linear regression, -0.002 min^{-1}, can be used to determine the true overall reaction constant in subsequent experiments defined later in this section. This value was determined to be adequate for further testing since it was less than 10% of the straight photolysis experiments performed at that time.

The photodegradation rate constant can now be determined. The following is the concentration profile of chlorobenzene once the reactor has been exposed to irradiation.

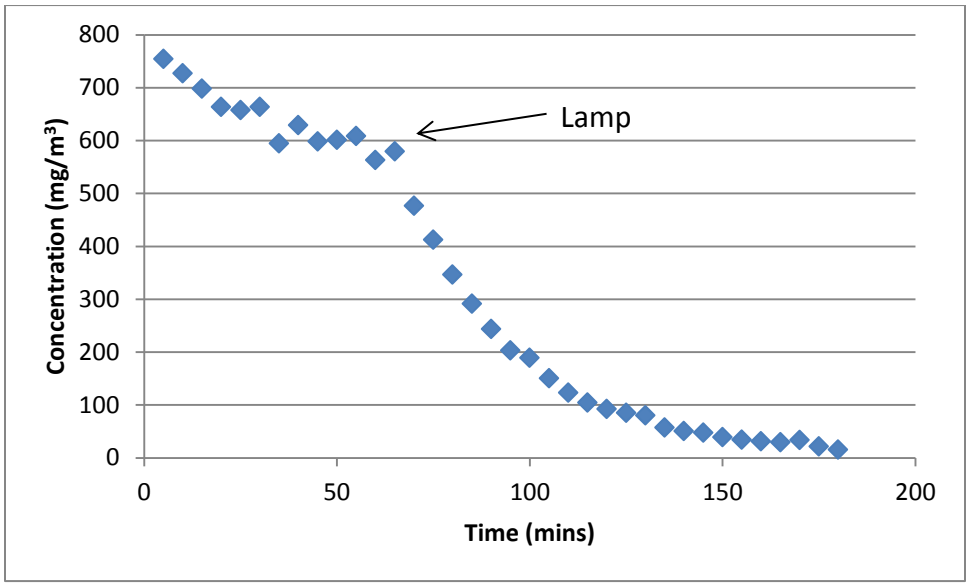

Figure 11. Chlorobenzene concentration profile versus time. Irradiation beginning at the 60 mins mark. Note the exponential decay after the lamp is turned on.

A first order reaction model was applied to the irradiation portion of the experiment. Figure 12 is the result of this approximation.

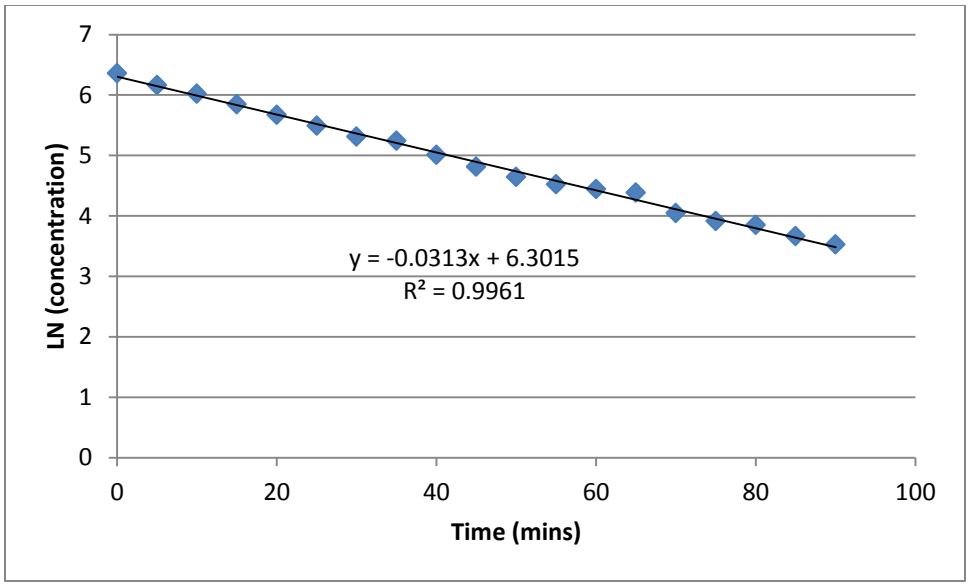

Figure 12. First order reaction model applied to irradiation. 15 uL injection, 30°C, 10% RH

A high coefficient of determination and a clearly linear relationship indicates the first order reaction model is accurate. The true reaction rate constant due to UV photolysis can be determined from the subtraction of the background degradation from the apparent reaction rate constant above. This relationship will hold true for all photolysis reactions.

$$\frac{dC}{dt} = -k_{UV}C - k_{other}C$$

$$\frac{dC}{dt} = -(k_{UV} + k_{other})C$$

$$k_{app} = k_{UV} + k_{other}$$

The following reaction pathways are likely some of the reactions involved after chlorobenzene absorbs a photo and becomes electronically excited (Dilmeghani & Zahir, 2001):

(24) $C_6H_5Cl + h\nu \rightarrow {}^{*}C_6H_5Cl$

(25) $C_6H_5Cl^{*} \rightarrow C_6H_5Cl + \text{heat}$

(26) $C_6H_5Cl^{*} \rightarrow \text{intermediates } (I_{UV})$

(27) $I_{UV} + h\nu \rightarrow {}^{*}I_{UV}$

(28) ${}^{*}I_{UV} \rightarrow \text{product(s)}$

5.3 Effect of Medium on Direct Photolysis

To determine the effects of the medium on straight photolysis, experiments were performed in a pure and dry nitrogen environment. This would effectively remove any effects oxygen or water vapour would have on the reaction mechanism leaving only the effects of UV irradiation and chlorobenzene produced radical reactions. Nitrogen was chosen as the reaction medium because of its inability to absorb germicidal radiation, that is, 254 nm. Nitrogen begins to absorb electromagnetic radiation at wavelengths below 125 nm ((J. Wang & Ray, 2000),(Chen et al., 2004). In Figure 13, the effect of temperature change on the reaction rate for both pure nitrogen and “dry” air (RH<10%) is shown.

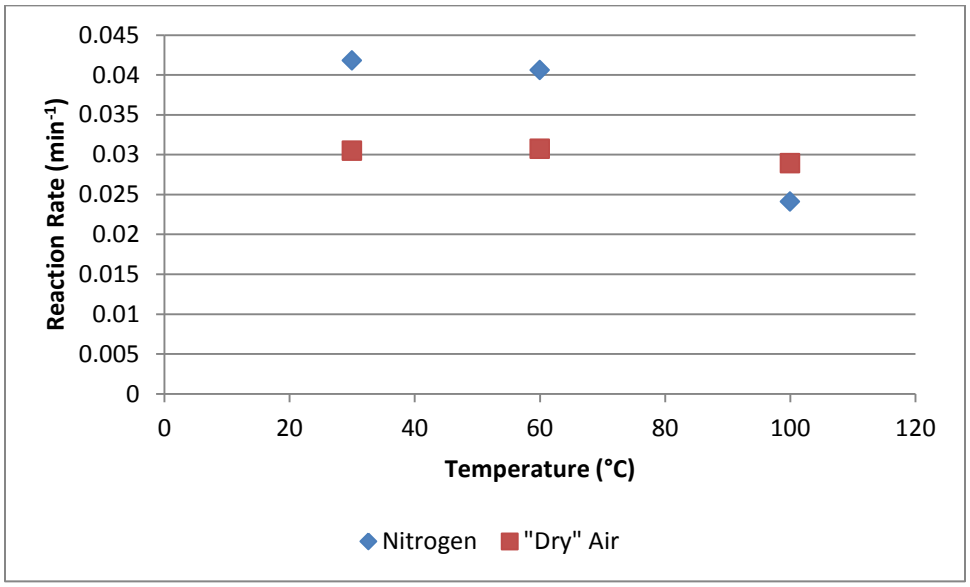

Figure 13. Reaction rate constants for photolysis reactions in dry air and nitrogen environments at 30°C.

The reaction rate is higher in the nitrogen medium for both 30°C and 60°C, but lower at 100°C. It would seem like the nitrogen plays some role in the radical reaction mechanism. In addition, this could be an indication of the effect of oxygen and water vapour on the reaction mechanism of chlorobenzene photolysis. This is in contrast to the data presented in Zhang and Anderson, for photolysis in a pure helium environment. In the helium environment, they noticed a decrease in the reaction rate as compared to the air environment. They reasoned that the phenyl and chlorine radicals produced from chlorobenzene photolysis react with water and

produce hydrogen radicals (Zhang & Anderson, 2013). The hydrogen radical then reacts with O_2 in the following ways (Dilmeghani & Zahir, 2001)(Huang & Shu, 1995)(Stone & Rowley, 2005):

(29) $O_2 + H^{\bullet} \rightarrow HO_2$

(30) $HO_2^{\bullet} + H^{\bullet} \rightarrow H_2O_2$

(16) $H_2O_2 + h\nu \rightarrow 2OH^{\bullet}$

(19) $HOO^{\bullet} + HOO^{\bullet} \rightarrow H_2O_2 + O_2$

However, there seems to be another mechanism in place in the nitrogen environment. A recent study by Shaffer et al. on the benzene dication has shown that this dication associates with molecular nitrogen to form a protonated diazonium and in the presence of water can form other aromatic dications (Shaffer, Schröder, Alcaraz, Žabka, & Zins, 2012).

5.4 Humidity and Temperature Effects

There have been a number of studies showing the positive effects of humidity on the degradation rates of volatile organic compounds. Water molecules can play an important role as reactants (J. Wang & Ray, 2000). Photolysis of the chlorobenzene molecule at the chlorine-carbon bond can produce phenyl and chlorine radicals (Dilmeghani & Zahir, 2001) (Da Silva, Vieira Ferreira, Machado, & Da Silva, 2006) A previous study by our group at a temperature of 25°C showed a positive effect of increased humidity from a relatively dry condition of 6.7% RH to wetter conditions of 46%. At a high humidity of 85% RH, there was no increase in the degradation rate from the 46% level (Lianfeng Zhang & Anderson, 2013).

Figure 14 shows all the compiled data for direct photolysis reactions for changes in humidity and temperature. All experiments had an injection of 15 µL of chlorobenzene at the beginning of the experiment. In terms of molar ratios, the humidity levels translate to 30:1, 120:1, and 210:1 water to chlorobenzene.

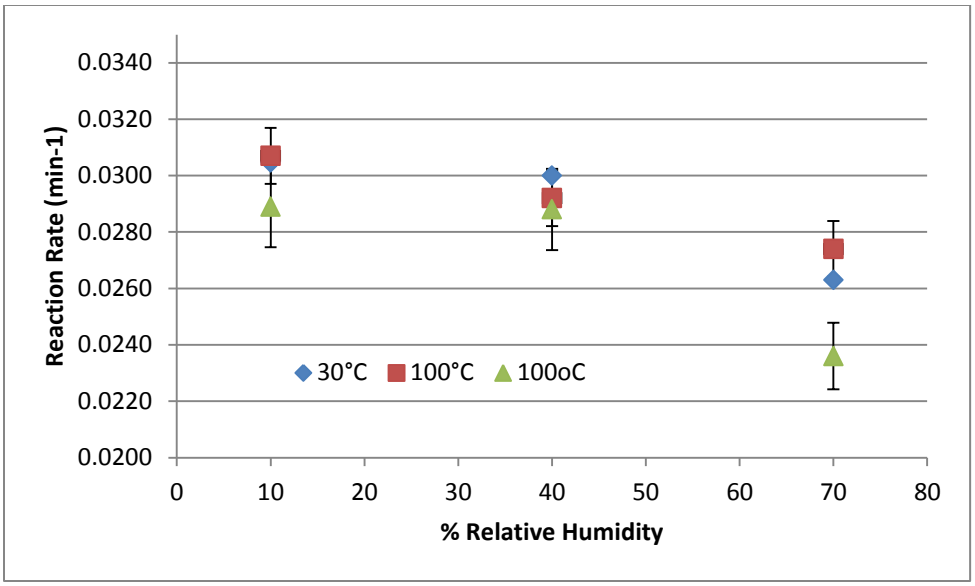

Figure 14. Influence of relative humidity on photolysis reaction rate constants at different temperatures. Error bars are one standard deviation based on replicates at 30°C and 10%RH.

At constant temperature, there is a detrimental effect of increased humidity. At the 70% relative humidity level the decrease in reaction rated dropped from a high of 0.0274 min^{-1} at 60°C to a low of 0.0236 min^{-1} at 100°C. The notion that increased water presence absorbed radiation intended for chlorobenzene photolysis does not hold true since water vapour does not begin to absorb UV radiation until 190 nm. This can be seen in Figure 15.

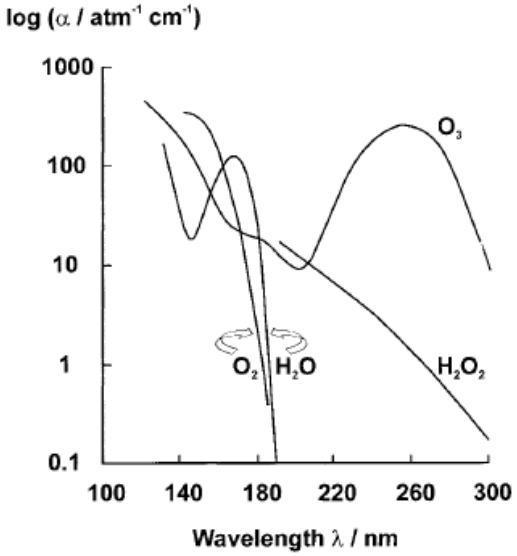

Figure 15. Absorption spectra for O_2, O_3, H_2O, and H_2O_2 in the gas phase. (Taken from (Oppenländer, 2003))

In a study by (Bhowmick & Semmens, 1994), the effect of moisture was evaluated on a number of different chlorinated alkanes and alkenes. The degradation rates for chloroform and 1,1,2-trichloroethane increased by 265% and 310% respectively in their study. This is from an extreme step change in relative humidity from 0% RH dry air to almost complete saturation, 95% RH. In a study by Wang et al (2009), their results indicated a possible relationship between an increase in humidity and the degradation rate of chlorobenzene. However, the interpretation of these results must be approached with caution since these studies employed low pressure mercury lamps with 185 nm radiation. Water vapour is known to have a continuous absorption spectrum from 175 to 190 nm and upon energy absorption can generate hydroxyl radicals (J. Wang & Ray, 2000):

(31) $$H_2O + h\nu \rightarrow H_2 + O(^3P) \text{ or } O(^1D)$$

32) $$H_2O + h\nu \rightarrow H^{\bullet} + OH^{\bullet}$$

For the direct photolysis scheme, it can be concluded that humidity has a negative impact on the degradation rate constants for all temperatures. This could be speculated that the water molecules are reacting with intermediate radicals after chlorobenzene photolysis. These intermediate radicals are potentially contributing to the chlorobenzene degradation in the absence of high levels of water molecules. The evidence for intermediate chain reactions can be seen in the quantum yield of the photolytic reaction which exceeds unity (Lianfeng Zhang & Anderson, 2013). More experiments should be performed to confirm this result.

5.5 Ozone Oxidation Experiments

A number of ozone and chlorobenzene experiments were performed to evaluate the photooxidation potential of chlorobenzene. Three different experiments were performed on each test level. All three of these reaction conditions accounted for the three main degradation pathways in the UV induced photo-reaction scheme. The first experiment was the background degradation of ozone at different humidity and temperature levels. This was to gauge the ozone loss due to difficult to account factors such as the reactor materials of construction and any unaccounted “contaminants” in the reactor. The second set of experiments determined the

reaction rate between ozone and chlorobenzene in the absence of ultraviolet radiation, in other words, ozonolysis of chlorobenzene. The third set of tests was the reaction between ozone and chlorobenzene in the presence of ultraviolet radiation. Knowing the results of the first two tests enables us to calculate the reaction rate of UV induced ozone photooxidation of chlorobenzene.

5.6 Ozone Degradation

For all of the experiments performed with ozone, the self-degradation rate of ozone was evaluated. This was to give an upper bound estimate to use in the UV/ozone experiments to account for the loss of ozone not attributed to photon absorption. The following graph shows the degradation rate of ozone in the reactor without any chlorobenzene or radiation present.

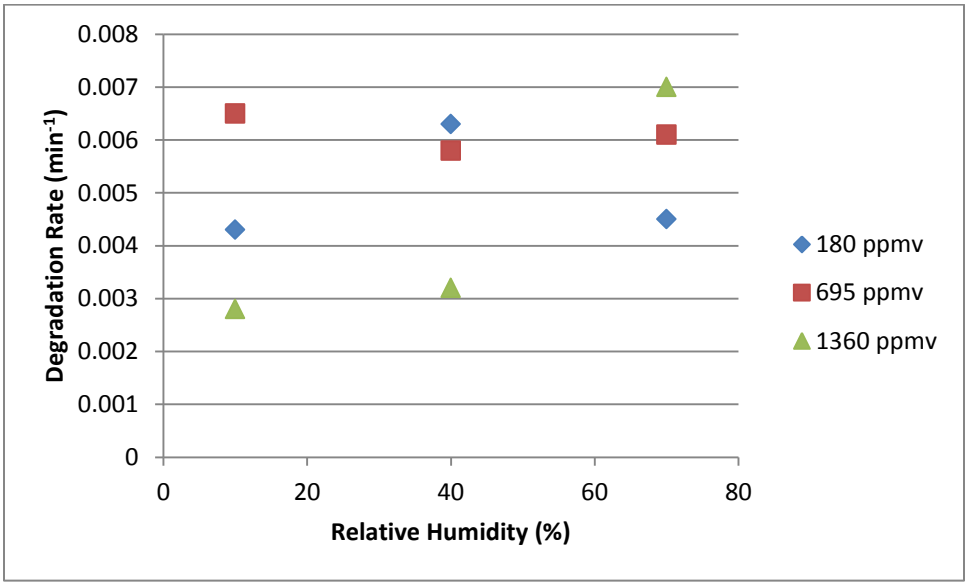

Figure 16. Ozone degradation rates in the absence of chlorobenzene at 30°C with no UV.

The data is a collection of three different starting concentrations of ozone and three different humidity levels at a constant temperature (30°C). There does not appear to be any correlation between the humidity level and ozone degradation due to the overlapping of trends for the different concentrations.

The temperature dependence of ozone degradation was also determined for the high and low humidity levels for the mid-level concentration level. There was a massive increase in

degradation from 30°C to 100°C, by over 7 times. This follows from theory as ozone is inherently unstable and will degrade according to the following mechanism (Benson & Axworthy, 1957):

(33) $$M + O_3 \leftrightharpoons M + O_2 + O$$

(34) $$O + O_3 \rightarrow 2O_2$$

The forward reaction of the first equation is temperature dependant (Benson & Axworthy, 1957) explaining the increase in degradation with temperature. This reaction has an activation energy to gas constant ration of 2060 K. Comparing reaction rates with the Arrhenius equation for 30 and 100°C, the expected increase in degradation should be approximately 3.6 (Sander et al., 2006). The fact that this research saw an increase of over 7 times could be indicative of other effects.

Other studies have shown ozone to be more thermally stable up to temperatures of 100°C for comparable concentrations(H. C. Wang et al., 2011)(Almquist, Sahle-Demessie, Sehker, & Sowash, 2007). The study by Wang et al., found something interesting about the degradation of ozone in the presence of iron oxide. In the presence of iron oxide, the group noticed that there was complete decomposition of ozone at 60°C (H. C. Wang et al., 2011). This is a strong indication that the reactor may have actually played a significant role in the degradation mechanism in this research since the top and bottom plates were made of steel, which is composed primarily of iron. The study by Wang et al. also went on to speculate on the reaction mechanism between the iron oxide, ozone, and chlorobenzene. They believed that the chlorobenzene is adsorbed onto the iron oxide through chlorine abstraction to form a surface phenolate (H. C. Wang et al., 2011), which corroborates an earlier study (Khaleel & Al-Nayli, 2008). The ozone in turn decomposes to form O^- on the catalyst surface and gaseous O_2 (H. C. Wang et al., 2011) (Oyama, 2000).

5.7 Ozonolysis Experiments

Due to the unstable nature of ozone it is known to be a strong oxidizing agent on its own. It is therefore important from a kinetic perspective to determine the extent of ozonolysis in the

present photoreactor system. For all experimental levels, based on humidity, temperature, and ozone concentration, the effect of ozonolysis was determined.

Ozonolysis was considered almost negligible at the 30°C level for all tests and humidity had no impact. However, there was a significant increase in the rate of ozonolysis with increasing reactor temperature.

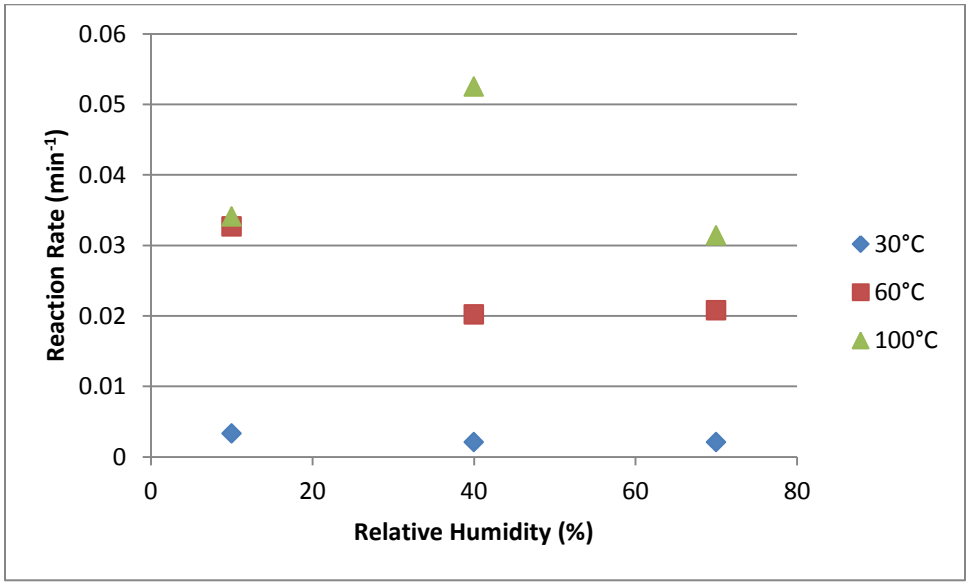

Figure 17. Effect of humidity and temperature on ozonoylsis for a 5:1 chlorobenzene to ozone molar ratio.

This may be due to an increase in the overall energy of the system. Increase in total energy will decrease the activation energy needed for a reaction to commence. Humidity seemed to have little to no effect on the reaction rates, except at the 100°C level and mid-range humidity. Other studies have also shown the minimum impact of humidity on the ozonolysis rate, albeit at lower operating temperatures (Shen & Ku, 1998)(Chou et al., 2005).

In general, the reaction rate between aromatics and ozone is rather slow. Chlorobenzene will react with ozone, but more slowly than other aromatics such as phenol. (Oyama, 2000) In general, ozone is a highly selective reagent and reactions with organics tend to be highly electrophilic (Rao & Chu, 2009). Interestingly, the reaction rates for 30°C are negligible compared to the UV/ozone rates, but the degradation rates for 60°C are very similar to those for the UV/O_3 process and at 100°C actually exceed those of the UV/O_3 process.

5.8 UV and Ozone Experiments

The use of ozone and ultraviolet has been shown many times over to drastically increase the degradation rate in a photochemical system. For all conditions described above, experiments of ozone coupled with ultraviolet light were performed. Chlorobenzene also absorbs at this wavelength, as the photolysis experiments showed, however the absorption coefficient is significantly less than that for ozone, at 139.6 L mol^{-1} cm^{-1} (Lianfeng Zhang & Anderson, 2013), and can be considered negligible for the concentration levels. The following table shows the degradation rate constants at 30°C at three different humidity levels and three different molar ratios between ozone and chlorobenzene.

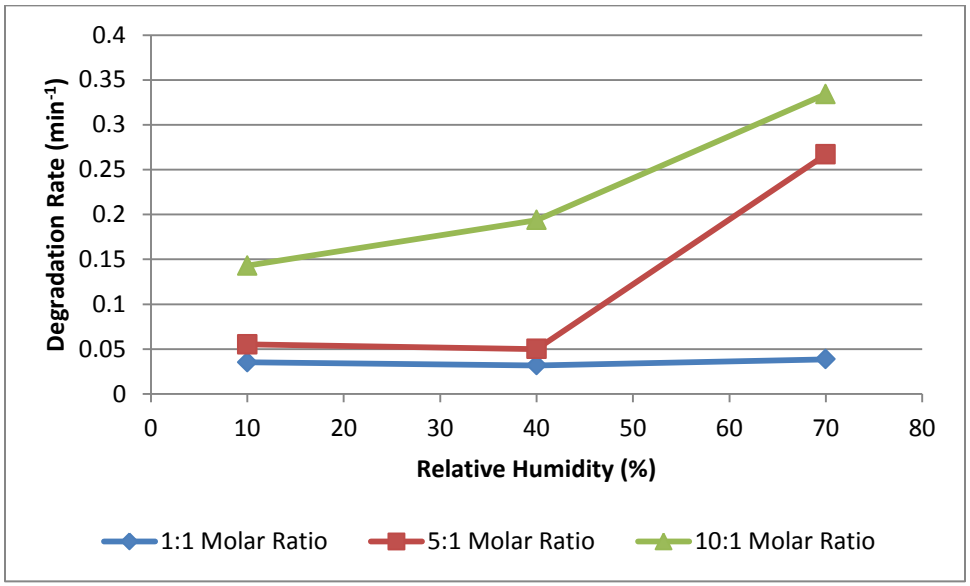

Figure 18. Global degradation constants of chlorobenzene in the presence of ozone and UV light at constant temperature of 30°C.

There is a marked increase in the degradation rate as the molar ratio increases. In addition, at the 5:1 and 10:1 molar ratio levels there is a positive correlation between the degradation rate and humidity level. Other studies how also found positive effects of increased ozone to target compound ratios (Chou et al., 2005)(Shen & Ku, 1998)(Yu & Lee, 2007). The study by Shen et al. noticed a slight decrease in reaction rates when ozone dosage increased passed a certain point, possibly due ozone molecules scavenging hydroxyl radicals destined for target compound

degradation and intermediate attack thus hindering the mineralization process (Shen & Ku, 1998). This could indicate major differences in reaction mechanisms.

This can be easily explained from the thoroughly established initiation mechanism of UV/Ozone photodegradation reactions. The oxygen radical produced from the initial UV absorption by ozone then needs to react with water molecules to produce hydroxyl radicals.

(1)	$O_3 + h\nu \rightarrow O_2 + O^{\bullet}$	(Shen & Ku, 1999)(Stone & Rowley, 2005) (Dunlea, Talukdar, & Ravishankara, 2005)
(2)	$O^{\bullet} + H_2O \rightarrow 2HO^{\bullet}$	(Chou et al., 2006)(Shen & Ku, 1999)(Dilmeghani & Zahir, 2001)(Stone & Rowley, 2005)(Dunlea et al., 2005)
(15)	$HO^{\bullet} + HO^{\bullet} \rightarrow H_2O_2$	(Dilmeghani & Zahir, 2001)
(16)	$H_2O_2 + h\nu \rightarrow 2HO^{\bullet}$	(Dilmeghani & Zahir, 2001)
(35)	$HO^{\bullet} + O_3 \rightarrow HO_2 + O_2$	(Lianfeng Zhang & Anderson, 2013)
(36)	$HO_2 + O_3 \rightarrow HO^{\bullet} + 2O_2$	(Lianfeng Zhang & Anderson, 2013)

At 1 atmosphere pressure and 298K, only about 10% of the $O(^1D)$ atoms react with water molecules to produce hydroxyl radicals even at 100% RH (Finlayson-Pitts & Pitts, 1986). Equation two will be in competition with the following reaction (Finlayson-Pitts & Pitts, 1986):

(3) $O(^1D) + M \rightarrow O(^3P) + M$

This is essentialy the electronic deactivation of $O(^1D)$ to $O(^3P)$ which does not have enough energy to produce radicals. In addition, there are two other significant reactions that can occur between the $O(^1D)$ and H_2O (Finlayson-Pitts & Pitts, 1986):

(4)	$O(^1D) + H_2O \rightarrow O(^3P) + H_2O$	(approximately 5%)
(5)	$O(^1D) + H_2O \rightarrow O_2 + H_2$	(approximately 1%)

In this investigation, there was a tremendous benefit for increased humidity, especially at the 100°C level. Other studies have found similar results of increased humidity on degradation rates (Chou et al., 2005)(Yu & Lee, 2007)(Pengyi et al., 2003).

The temperature dependence of the UV/Ozone process was also investigated for the mid-level molar ratio, due to the extremely fast degradation kinetics of the 10:1 molar ratio experiments. These results can be seen in Figure 19.

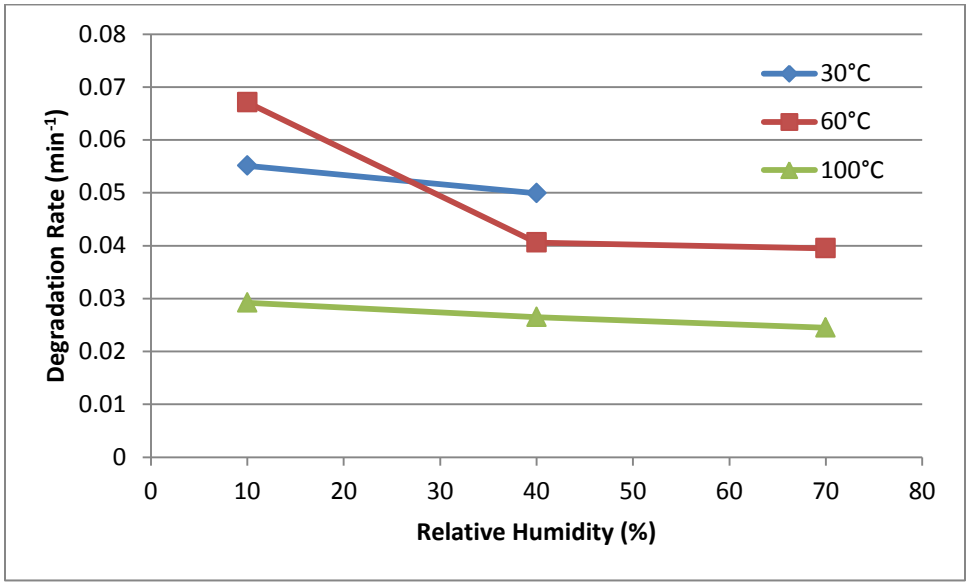

Figure 19. Effect of temperature on the UV/ozone degradation of chlorobenzene for a 5:1 ozone to chlorobenzene ratio. The value at 30°C and 70%RH has been removed to emphasize the trends.

There was a noticeable decrease in the reaction rate as the temperature of the reactor increased. This may be due to the effects of ozone self-degradation increasing at a higher temperature, as seen in the ozonolysis experiments, and thus not absorbing enough UV radiation to produce hydroxyl radicals. The reaction rate constant for 30°C and 5:1 ozone to chlorobenzene seems to be an outlier and was removed from Figure 19. However, in the previous figure, Figure 18, the degradation rate seems reasonable as compared to the other rates for that temperature. This could indicate the competing nature of the ozone reactions. As mentioned in the ozonolysis experiments, the rates are rather negligible at the lower temperatures. However the rates found in the ozonolysis reactions and the rates found in the UV/ozone scheme begin to converge as temperature increases at a constant molar ratio of 5:1. Ozonolysis rates were higher than the UV/Ozone rates at the 100°C level. It would seem that temperature plays an important role in the UV/Ozone reactions in hindering the degradation rate as compared to ozonolysis reactions.

The study by Shen and Ku investigated the temperature effect on UV/Ozone treatment of chloroethenes and found there was no significant effects for the temperature range 25 to 65°C (Shen & Ku, 1998).

5.9 UV and H_2O_2 Experiments

Experiments with hydrogen peroxide were performed of an exploratory nature due to the difficulties in introducing H_2O_2 into the gas phase. To ensure complete dispersion of the H_2O_2 aerosols the aerosol feed was flowed through the reactor for 30 minutes at an approximate flow rate of 11.5 L/min while the recirculation pump was turned on. Due to the nature of the application method of the H_2O_2 it can be assumed that the reactor was fully saturated with water as well. Figure 20 shows the concentration profile of chlorobenzene in the presence of H_2O_2 and UV light.

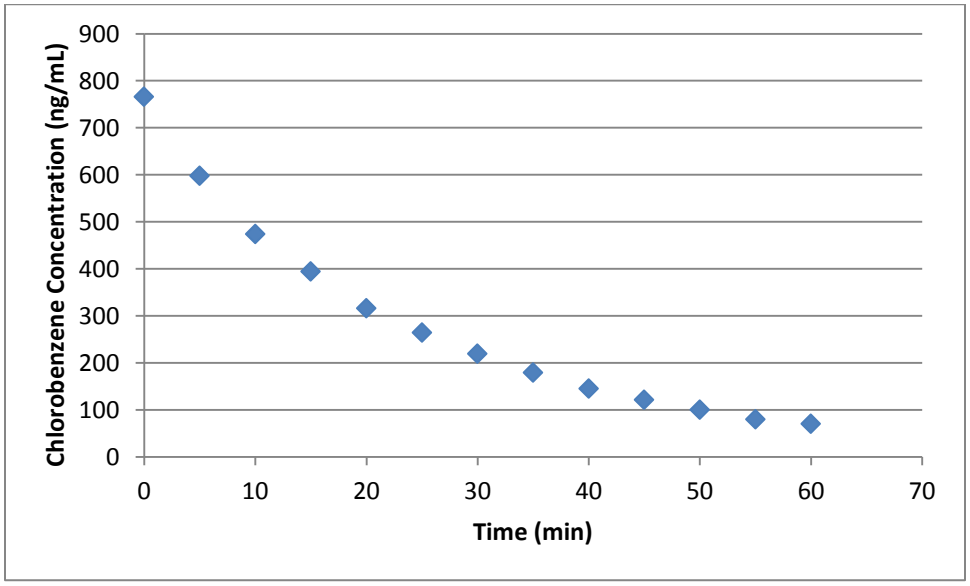

Figure 20. Chlorobenzene concentration profile in the presence of H_2O_2 and UV light at 30°C.

The regressed degradation constant from this experiment was -0.0397 min^{-1}. This degradation rate compares quite favorably to that of direct photolysis with an approximate increase of 40% at the closest level for direct photolysis of 30°C and 70%RH. However, it was significantly lower as compared to the UV/O_3. This can be easily explained from the relative absorption

coefficients of O_3 and H_2O_2 at 254 nm. As seen earlier, when O_3 absorbs a photon the following reactions occur:

(1) $O_3 + h\nu \rightarrow O_2 + O^{\bullet}$

(2) $O^{\bullet} + H_2O \rightarrow 2HO^{\bullet}$

However, when hydrogen peroxide absorbs a photon the following reaction occurs:

(16) $H_2O_2 + h\nu \rightarrow 2HO^{\bullet}$

It would seem that from a mechanistic point of view, the hydrogen peroxide reaction would be more favourable and this is indeed true for the aqueous phase where much higher concentrations of H_2O_2 can be achieved than O_3, because of its solubility limitation. However, the absorption coefficient for hydrogen peroxide is only about 18.7 L mol^{-1} cm^{-1} as compared to the absorption coefficient for ozone of 3020 L mol^{-1} cm^{-1}. Clearly many more ozone molecules will be participating in reactions than hydrogen peroxide molecules and this can be seen from the quantum yields of both reactions. For the ozone photodecomposition, it is about 0.1. For H_2O_2, it is about 1.0 but since ozone's absorption is more than 10 times higher than H_2O_2 it is still more favorable (Bolton & Cater, 1994).

Interesting enough, the absorption coefficient for chlorobenzene is 139.6 L mol^{-1} cm^{-1} at 254 nm. This is almost 6.5 times higher than the absorption coefficient of H_2O_2. The photolysis reaction likely contributes the most to the overall reaction rate, but the positive impact of the H_2O_2 cannot be ignored.

Further experiments would have been performed with this reaction scheme, but due to the nature of hydrogen peroxide delivery into the reactor this proved difficult. Concentration stability proved extremely difficult to achieve after a handful of experiments were performed. This was most likely due to the hydrogen peroxide condensing on the walls of the reactor and possibly engaging in reactions with any species adsorbed onto the walls. This was not as pronounced with the ozone experiments possibly due to the fact that ozone maintained its gaseous state and was not in intimate contact with the reactor walls as the condensate would

have been. A continuous flow reactor would prove better in H_2O_2 testing and higher reactor temperatures may reduce the condensation issues.

6.0 Conclusions

The reactor materials proved to be very troublesome in performing experiments. A number of background tests were performed to establish interactions between chlorobenzene and the materials of construction and resulted in unpredictable concentration profiles. The predicted level and straight profiles were only seen in a small number of experiments. These types of conditions would most likely been seen in practical applications; air handling systems in the intended applications would be composed of steel and similar materials. The research underlines the complexities of implicating UV technologies in industrial settings.

Nitrogen was shown to play an important part in the direct photolysis degradation reactions at temperatures of 20 and 60°C. Temperature did not influence the degradation rate in direct photolysis of chlorobenzene as expected from literature.

Temperature and humidity were not greatly influential on the degradation rates of direct photolysis. The degradation rate of chlorobenzene at a temperature of 100°C and high humidity was noticeably reduced, but unchanged at the 10% RH and 60% RH levels for all temperatures.

Ozone only experiments showed ozone degradation at low temperatures. Some studies report ozone to be thermally stable at temperatures up to 150°C. This may indicate unaccounted species on the reactor walls that react with the ozone molecules. Although efforts were made to cleanse the reactor between experiments, non-volatile and non-polar by-products of the degradation reactions may have remained.

Ozonolysis of chlorobenzene was negligible at 30°C for all humidity levels. Ozonolysis reactions at the 60°C and 100°C levels were as higher than direct photolysis rates and in the 100°C case exceeded the UV/O_3 degradation rates.

Ozone coupled with UV experiments proved to be the most destructive at the low temperature of 30°C. There was a clear and positive relationship between the amount of ozone present in the reactor and the degradation rate. At lower ozone to chlorobenzene molar ratios the degradation rates were not much higher than those for direct photolysis of ozone. The fastest degradation rate was achieved for the 10:1 molar ratio and high humidity, which was over 10

times the rate of direct photolysis. In addition humidity was noticeably important in these reactions.

The effect of temperature on the UV/ozone reaction scheme was determined for the 5:1 ozone to chlorobenzene ratio. Temperature had an interesting effect on the degradation rates at higher temperatures. As the reactor temperature increased, the degradation rates from ozonolysis and UV/O_3 began to converge, ultimately leading to the ozonolysis reaction being faster than the UV/O_3.

Exploratory reactions experiments for the H_2O_2 scheme were performed. H_2O_2 had a positive influence on the degradation rate of chlorobenzene and was about 26% higher than the direct photolysis rates. However for similar conditions, the UV/O_3 process had higher degradation rates as was expected from the difference in absorption values between ozone and hydrogen peroxide. Although difficulties exist in introducing H_2O_2 into the gas phase, these technical limitations have been sufficiently solved in other studies using injection nozzles (Cooper, Clausen, Pettey, Collins, & Fernandez, 2002) (Cooper, Clausen, Pettey, Muller, & Collins, 2002).

In terms, of PCDD/PCDF destruction potential it would seem that the UV/O_3 process has promise. PCDD/PCDFs are present in smaller amounts in the exhausts of the source processes than those employed in this study and as such the processes evaluated should be able to effectively destroy these compounds.

7.0 Recommendations

I. *Determine the exact nature of the interactions between the reactor materials and chlorobenzene.*

One major difficulty in this research was attaining repeatability in results due to unknown interactions with the reactor walls. If further studies are to be conducted with chlorobenzene (and likely other halogenated aromatics), the relationship between the reactor materials and the reactants must be determined. From an industrial application perspective this is extremely important as well since the materials of construction will be similar (steel or aluminum). Unaccounted for reactions my produce undesirable by-products that may potentially be as harmful or more so than the target polluntants. On the other hand, if the mechanism is simply adsorption, then the issue of pollutant destruction is not actually solved, but rather just transferred to a different phase.

II. *Product identification for the UV/O_3 and ozonolysis processes at higher temperatures to determine if there are changes in the degradation mechanism.*

There have been some studies attempting to identify the by-products of direct photolysis and UV/O_3 (C. Wang, Xi, & Hu, 2008)(Dilmeghani & Zahir, 2001)(L Zhang et al., 2007). However, these analyses were at low temperatures. Similar analyses should be undertaken at higher temperatures to better elucidate the mechanism of degradation and to verify complete mineralization of organic compounds.

III. *Further testing with H_2O_2 at higher reaction temperatures and lower irradiance wavelengths.*

Evidence from the ozonolysis and UV/O_3 experiments show that temperature is important when ozone is involved in the degradation reactions. It is widely known that H_2O_2 begins to thermally degrade at 500°C, but studies have shown that even significantly below these temperatures there exists a positive temperature relationship with the UV/H_2O_2 process (Cooper, Clausen, Pettey, Collins, et al., 2002). In the UV/O_3 process temperature proved

detrimental, whereas temperature may prove beneficial for the UV/H_2O_2 process in the present system.

Bibliography

Abad, E., Caixach, J., & Rivera, J. (2003). Improvements in dioxin abatement strategies at a municipal waste management plant in Barcelona. *Chemosphere*, *50*(9), 1175–82.

Alcock, R. E., & Jones, K. C. (1996). Dioxins in the Environment: A Review of Trend Data. *Environmental Science & Technology*, *30*(11), 3133–3143. doi:10.1021/es960306z

Almquist, C. B., Sahle-Demessie, E., Sehker, K. S. C., & Sowash, J. (2007). Methanol oxidation using ozone on titania-supported vanadia catalyst. *Environmental science & technology*, *41*(13), 4754–60.

Anderson, D. R., & Fisher, R. (2002). Sources of dioxins in the United Kingdom: the steel industry and other sources. *Chemosphere*, *46*(3), 371–81.

Benson, S. W., & Axworthy, A. E. (1957). Mechanism of the Gas Phase, Thermal Decomposition of Ozone. *The Journal of Chemical Physics*, *26*(6), 1718. doi:10.1063/1.1743610

Bhowmick, M., & Semmens, M. J. (1994). Ultraviolet photooxidation for the destruction of vocs in air. *Water Research*, *28*(11), 2407–2415. doi:10.1016/0043-1354(94)90057-4

Bolton, J. R., & Cater, S. R. (1994). Homogeneous Photodegradation of Pollutants in Contaminated Water: An Introduction. *Aquatic and surface photochemistry*. Boca Raton: Lewis Publishers.

Carlos, A., Brandi, M. R. J., & Alfanot, O. M. (1996). Photoreactor Analysis and Design : Fundamentals and Applications. *Industrial & Engineering Chemistry Research*, 2155–2201.

Chen, F., Yang, Q., Pehkonen, S. O., & Ray, M. B. (2004). Modeling of gas-phase photodegradation of chloroform and carbon tetrachloride. *Journal of the Air & Waste Management Association (1995)*, *54*(10), 1281–92.

Choi, W., Hong, S. J., Chang, Y.-S., & Cho, Y. (2000). Photocatalytic Degradation of Polychlorinated Dibenzo- p -dioxins on TiO 2 Film under UV or Solar Light Irradiation. *Environmental Science & Technology*, *34*(22), 4810–4815. doi:10.1021/es0011461

Chou, M.-S., Huang, B.-J., & Chang, H.-Y. (2005). Decomposition of gas phase 1,3-butadiene by ultraviolet/ozone process. *Journal of the Air & Waste Management Association (1995)*, *55*(7), 919–29.

Chou, M.-S., Huang, B.-J., & Chang, H.-Y. (2006). Degradation of gas-phase propylene glycol monomethyl ether acetate by ultraviolet/ozone process: A kinetic study. *Journal of the Air & Waste Management Association (1995)*, *56*(6), 767–76.

Choudhry, G. G., & Webster, G. R. B. (1989). Environmental Photochemistry of PCDDs . 2 . Quantum Yields of the Direct Phototransformation of 1,2,3,7-Tetra-, 1,3,6,8-Tetra-, 1,2,3,4,6,7,8-Hepta-, and 1,2,3,4,6,7,8,9-Octachlorodibenzo-p-dioxin in Aqueous Acetonitrile and Their Sunlight Half -Lives. *Journal of Agricultural and Food Chemistry*, *1*(1), 254–261.

Cieplik, M. K., Carbonell, J. P., Muñoz, C., Baker, S., Krüger, S., Liljelind, P., Marklund, S., et al. (2003). On dioxin formation in iron ore sintering. *Environmental science & technology*, *37*(15), 3323–31.

Cooper, C. D., Clausen, C. A., Pettey, L., Collins, M. M., & Fernandez, M. P. de. (2002). Investigation of Ultraviolet Light-Enhanced H2O2 Oxidation of NOx Emissions. *Journal of Environmental Engineering*, *128*(1), 68–72.

Cooper, C. D., Clausen, C. a., Pettey, L., Muller, P., & Collins, M. M. (2002). Injection Nozzle for Ultraviolet Light-Enhanced H2O2 Oxidation of Air Pollutants in Flue Gas. *Journal of Environmental Engineering*, *128*(12), 1175. doi:10.1061/(ASCE)0733-9372(2002)128:12(1175)

Crosby, D. G., Moilanen, K. W., & Wong, A. S. (1973). Environmental Generation and Degradation of Dibenzodioxins and Dibenzofurans. *Environmental Health Perspectives*, *5*(September), 259–266.

Cudahy, J. J., & Helsel, R. W. (2000). Removal of products of incomplete combustion with carbon. *Waste Management*, *20*(5-6), 339–345. doi:10.1016/S0956-053X(99)00335-9

Da Silva, J. P., Vieira Ferreira, L. F., Machado, I. F., & Da Silva, A. M. (2006). Photolysis of 4-chloroanisole in the presence of oxygen. *Journal of Photochemistry and Photobiology A: Chemistry*, *182*(1), 88–92. doi:10.1016/j.jphotochem.2006.01.019

Dickson, L. C., Lenoir, D., & Hutzinger, O. (1992). Quantitative Comparison of de Novo and Precursor Formation of Polychlorinated Dibenzo-p-dioxins under Simulated Municipal Solid Waste Incinerator Postcombustion Conditions. *Environmental Science & Technology*, *26*(9), 1822–1828.

Dilmeghani, M., & Zahir, K. O. (2001). Kinetics and Mechanism of Chlorobenzene Degradation in Aqueous Samples Using Advanced Oxidation Processes. *Journal of Environmental Quality*, *30*(6), 2062–2070.

Dobbs, A. J., & Grant, C. (1979). Photolysis of highly chlorinated dibenzo-p-dioxins by sunlight. *Nature*, (278), 163–165.

Dunlea, E. J., Talukdar, R. K., & Ravishankara, a R. (2005). Kinetic studies of the reactions of O2(b 1sigma(g)+) with several atmospheric molecules. *The journal of physical chemistry. A*, *109*(17), 3912–20. doi:10.1021/jp044129x

Environment Canada. (2012). *2010 NPRI Reviewed Facility Data Release*.

Everaert, K., & Baeyens, J. (2004). Catalytic combustion of volatile organic compounds. *Journal of hazardous materials*, *109*(1-3), 113–39. doi:10.1016/j.jhazmat.2004.03.019

Everaert, K., Basyens, J., & Degrève, J. (2002). Removal of PCDD/F from incinerator flue gases by entrained-phase adsorption. *Journal of the Air & Waste Management Association (1995)*, *52*(12), 1378–88.

Feiyan, C., Pehkonen, S. O., & Ray, M. B. (2002). Kinetics and mechanisms of UV-photodegradation of chlorinated organics in the gas phase. *Water research*, *36*(17), 4203–14.

Finlayson-Pitts, B. J., & Pitts, J. N. J. (1986). *Atmospheric Chemistry: Fundamentals and experimental techniques*. New York, NY: John Wiley and Sons.

Finocchio, E., Busca, G., & Notaro, M. (2006). A review of catalytic processes for the destruction of PCDD and PCDF from waste gases. *Applied Catalysis B: Environmental*, *62*(1-2), 12–20. doi:10.1016/j.apcatb.2005.06.010

Gerasimov, G. Y. (2001). Degradation of Dioxins in Electron-Beam Gas Cleaning of Sulfur and Nitrogen Oxides. *High Energy Chemistry*, *35*(6), 427–431.

Glaze, W. H., Kang, J., & Douglas, H. (1987). The Chemistry of Water Treatment Processes Involving Ozone , Hydrogen Peroxide and Ultraviolet Radiation. *Ozone: Science & Engineering*, *9*(4), 335–352.

Glaze, W. H., Peyton, G. R., Lin, S., Huang, R. Y., & Burieson, J. L. (1982). Destruction of Pollutants in Water with Ozone in Combination with Ultraviolet Radiation. 2. Natural Trihalomethane Precursors. *Environmental Science & Technology*, *16*(8), 454–458.

Goemans, M., Clarysse, P., Joannès, J., De Clercq, P., Lenaerts, S., Matthys, K., & Boels, K. (2004). Catalytic NOx reduction with simultaneous dioxin and furan oxidation. *Chemosphere*, *54*(9), 1357–65. doi:10.1016/S0045-6535(03)00255-8

Government of Canada. (2006a). Canada's National Implementation Plan under the Stockholm Convention on Persistent Organic Pollutants. Ottawa, Ontario, Canada: Government of Canada.

Government of Canada. (2006b). *Canada's National Implementation Plan under the Stockholm Convention on Persistent Organic Pollutants*. Ottawa, Ontario, Canada.

Grammaticakis, P. (1949). Contribution a l'etude de l'absorption dans l'ultraviolet moyen des anilines orthosubstituees. II. Ortho-halogenanilines N-substituees. *Bulletin de la Société Chimique de France*, (16), 761.

Haag, W. R., Johnson, M. D., & Scofield, R. (1996). Direct Photolysis of Trichloroethene in Air: Effect of Cocontaminants, Toxicity of Products, and Hydrothermal Treatment of Products. *Environmental Science & Technology*, *30*(2), 414–421. doi:10.1021/es950047y

Hoigne, J., & Bader, H. (1983). Rate Constants of Reactions of Ozone with Organic and Inorganic Compounds in Water - I: Non-Dissociating Organic Compounds. *Water Research*, *l*, 173–183.

Huang, C.-R., & Shu, H. Y. (1995). The reaction kinetics, decomposition pathways and intermediate formations of phenol in ozonation, UV/O3 and UV/H2O2 processes. *Journal of Hazardous Materials*, *41*(1), 47–64.

Hung, L., & Ingram, L. L. (1990). Effect of Solvents on the Photodegradation Rates of Octachlorodibenzo-p-dioxin. *Bulletin of Environmental Contamination and Toxicology*, *44*(3), 380–386.

Hutzinger, O., Safe, S., Wentzell, B. R., & Zitkhe, V. (1973). Photochemical Degradation of Di- and Octachiorodibenzofuran. *Environmental Health Perspectives*, *5*(September), 267–271.

Jeong, J., Sekiguchi, K., & Sakamoto, K. (2004). Photochemical and photocatalytic degradation of gaseous toluene using short-wavelength UV irradiation with TiO2 catalyst: comparison of three UV sources. *Chemosphere*, *57*(7), 663–71. doi:10.1016/j.chemosphere.2004.05.037

Karademir, A., Bakoğlu, M., & Ayberk, S. (2003). PCDD/F Removal Efficiencies Of Electrostatic Precipitator And Wet Scrubbers In Izaydas Hazourdous Waste Incinterator. *Fresenius Environmental Bulletin*, *12*(10), 1228–1232.

Khaleel, A., & Al-Nayli, A. (2008). Supported and mixed oxide catalysts based on iron and titanium for the oxidative decomposition of chlorobenzene. *Applied Catalysis B: Environmental*, *80*(1-2), 176–184. doi:10.1016/j.apcatb.2007.11.027

Kulkarni, P. S., Crespo, J. G., & Afonso, C. a M. (2008). Dioxins sources and current remediation technologies--a review. *Environment international*, *34*(1), 139–53. doi:10.1016/j.envint.2007.07.009

Lavric, E. D., Konnov, A. a, & De Ruyck, J. (2005). Surrogate compounds for dioxins in incineration. A review. *Waste management (New York, N.Y.)*, *25*(7), 755–65. doi:10.1016/j.wasman.2004.12.026

Lavric, E. D., Konnov, A. a., & Ruyck, J. De. (2004). Dioxin levels in wood combustion—a review. *Biomass and Bioenergy*, *26*(2), 115–145. doi:10.1016/S0961-9534(03)00104-1

Lee, K. Y., & Lee, J. (2005). Photochemical Destruction of Tetrachloroethylene and Trichloroethylene from the Exhaust of an Air Stripper, (October), 1441–1446.

Liljelind, P., Unsworth, J., Maaskant, O., & Marklund, S. (2001). Removal of dioxins and related aromatic hydrocarbons from flue gas streams by adsorption and catalytic destruction. *Chemosphere*, *42*(5-7), 615–23.

Mackay, D., Shiu, W. Y., Ma, K., & Lee, S. C. (2006). Volume 2 Halogenated Hydrocarbons. *Physical-Chemical Properties and Environmental Fate for Organic Chemicals* (Second Edi., Vol. III). Boca Raton: CRC Press.

Marinković, N., Pašalić, D., Ferenčak, G., Gršković, B., & Stavljenić Rukavina, A. (2010). Dioxins and human toxicity. *Arhiv za higijenu rada i toksikologiju*, *61*(4), 445–53. doi:10.2478/10004-1254-61-2010-2024

Miller, G. C., Hebert, R., Miille, M. J., Mitzel, R., & Zepp, R. G. (1989). Photolysis of Octachlorodibenzo-p-dioxin on Soils: Production of 2,3,7,8-tcdd. *Chemosphere*, *18*(1-6), 1265–1274.

Mitrou, P. I., Dimitriadis, G., & Raptis, S. a. (2001). Toxic effects of 2,3,7,8-tetrachlorodibenzo-p-dioxin and related compounds. *European journal of internal medicine*, *12*(5), 406–411.

Olie, K., Vermeulen, P., & Hutzinge, D. (1977). Chlorobenzo-p-dioxins and chlorodibenzofurans are trace components of fly ash and flue gas of some municipal incinerators in the Netherlands. *Chemosphere*, *6*(8), 455–459.

Oppenländer, T. (2003). *Photochemical Purification of Water and Air*. Frankfurt: Wiley-VCH.

Oyama, S. T. (2000). Chemical and Catalytic Properties of Ozone. *Catalysis Reviews*, *42*(3), 279–322. doi:10.1081/CR-100100263

Pengyi, Z., Fuyan, L., Gang, Y., Qing, C., & Wanpeng, Z. (2003). A comparative study on decomposition of gaseous toluene by O3/UV, TiO2/UV and O3/TiO2/UV. *Journal of Photochemistry and Photobiology A: Chemistry*, *156*(1-3), 189–194. doi:10.1016/S1010-6030(02)00432-X

Quass, U., Fermann, M., & Bröker, G. (2004). The European dioxin air emission inventory project--final results. *Chemosphere*, *54*(9), 1319–27. doi:10.1016/S0045-6535(03)00251-0

Rabek, J. F. (1982). *Experimental Methods in Photochemistry and Photophysics, Part 2.* Toronto: John Wiley & Sons Ltd.

Rao, Y. F., & Chu, W. (2009). A new approach to quantify the degradation kinetics of linuron with UV, ozonation and UV/O3 processes. *Chemosphere*, *74*(11), 1444–9. doi:10.1016/j.chemosphere.2008.12.012

Ray, M. B. (2000). Photodegradation of the Volatile Organic Compounds in the Gas Phase : A Review, *8*, 405–439.

Sander, S. P., Friedl, R. R., Golden, D. M., Kurylo, M. J., Moortgat, G. K., Wine, P. H., Ravishankara, A. R., et al. (2006). *Chemical Kinetics and Photochemical Data for Use in Atmospheric Studies Evaluation Number 15*.

Shaffer, C. J., Schröder, D., Alcaraz, C., Žabka, J., & Zins, E.-L. (2012). Reactions of doubly ionized benzene with nitrogen and water: a nitrogen-mediated entry into superacid chemistry. *Chemphyschem : a European journal of chemical physics and physical chemistry*, *13*(11), 2688–98. doi:10.1002/cphc.201200313

Shen, Y.-S., & Ku, Y. (1998). Decomposition of gas-phase chloroethenes by UV/O3 process. *Water Research*, *32*(9), 2669–2679. doi:10.1016/S0043-1354(98)00045-1

Shen, Y.-S., & Ku, Y. (1999). Treatment of Gas-Phase Volatile Organic Compounds (VOCs) by the UV/O3 Process. *Chemosphere*, *38*(8), 1855–1866.

Shiomitsu, T., Hirayama, A., Iwasaki, T., Akashi, T., & Fujisawa, Y. (2002). Volatilization and Decomposition of Dioxin from Fly Ash with Agitating Fluidized Bed Heating Chamber. *NKK Technical Review*, *86*(86), 1–5.

Stone, D., & Rowley, D. M. (2005). Kinetics of the gas phase HO2 self-reaction: effects of temperature, pressure, water and methanol vapours. *Physical chemistry chemical physics : PCCP*, *7*(10), 2156–63.

Travis, C. C., & Hattemer-Frey, H. A. (1991). Human exposure to dioxin. *The Science of the Total Environment*, *104*(1991), 97–127.

Tysklind, M., Lindskog, A., Thaning, L., Rappet, C., & Defence, N. (1993). Atmospheric Transport and Transformation of Polychlorinated Dibenzo-pdioxins and Dibenzofurans, (12), 2190–2197.

UNEP. (2005). *Ridding the World of POPs: A Guide to the Stockholm Convention*.

UNEP. (2007). *Guidelines on best available techniques and provisional guidance on best environmental practices relevant to article 5 and annex c of the stockholm convention on persistent organic pollutants Introduction : Sections I-IV*.

Wagenaar, W. J., Boelhouwers, E. J., De Kok, H. A. M., & Groen, C. P. (1995). A Comparative Study of the Photolytic Degradation of Octachlorodibenzofuran (OCDF) and Octachlorodibenzo-p-dioxin (OCDD). *Chemosphere*, *31*(4), 2983–2992.

Wang, C., Xi, J., & Hu, H. (2008). Chemical identification and acute biotoxicity assessment of gaseous chlorobenzene photodegradation products. *Chemosphere*, *73*(8), 1167–71. doi:10.1016/j.chemosphere.2008.07.065

Wang, H. C., Liang, H. S., & Chang, M. B. (2011). Ozone-enhanced catalytic oxidation of monochlorobenzene over iron oxide catalysts. *Chemosphere*, *82*(8), 1090–5. doi:10.1016/j.chemosphere.2010.12.046

Wang, J., & Ray, M. B. (2000). Application of ultraviolet photooxidation to remove organic pollutants in the gas phase. *Separation and Purification Technology*, *19*(1-2), 11–20. doi:10.1016/S1383-5866(99)00078-7

Wang, L.-C., Lee, W.-J., Tsai, P.-J., Lee, W.-S., & Chang-Chien, G.-P. (2003). Emissions of polychlorinated dibenzo-p-dioxins and dibenzofurans from stack flue gases of sinter plants. *Chemosphere*, *50*(9), 1123–9.

Wekhof, A. (1991). Treatment of contaminated water, air, and soil. *Environmental Progress*, *10*(4), 241–247.

Yu, K., & Lee, G. (2007). Decomposition of gas-phase toluene by the combination of ozone and photocatalytic oxidation process (TiO2/UV, TiO2/UV/O3, and UV/O3). *Applied Catalysis B: Environmental*, *75*(1-2), 29–38. doi:10.1016/j.apcatb.2007.03.006

Zhang, L, Sawell, S., Moralejo, C., & Anderson, W. (2007). Heterogeneous photocatalytic decomposition of gas-phase chlorobenzene. *Applied Catalysis B: Environmental*, *71*(3-4), 135–142. doi:10.1016/j.apcatb.2006.08.016

Zhang, Lianfeng, & Anderson, W. A. (2013). Kinetic analysis of the photochemical decomposition of gas-phase chlorobenzene in a UV reactor: Quantum yield and photonic efficiency. *Chemical Engineering Journal*, *218*, 247–252. doi:10.1016/j.cej.2012.12.004